

2. EXPLANATORY NOTES¹

Shipboard Scientific Party²

INTRODUCTION

This chapter contains information that will help the reader understand the basis for our preliminary conclusions and also help the interested investigator select samples for further analysis. This information concerns only shipboard operations and analyses described in the site reports in the *Initial Results* volume of the Leg 144 *Proceedings of the Ocean Drilling Program*. Methods used by various investigators for shore-based analyses of Leg 144 data will be detailed in the individual scientific contributions published in the *Scientific Results* volume.

Authorship of Site Chapters

The separate sections of the site chapters were written by the following shipboard scientists (authors are listed in alphabetical order, no seniority is necessarily implied):

Principal Results: Haggerty, Premoli Silva
Background and Objectives: Haggerty, Premoli Silva
Operations: Foss, Haggerty
Underway and Site Geophysics: Bergersen
Lithostratigraphy: Bogdanov, Camoin, Enos, Jansa, Lincoln, Quinn
Biostratigraphy: Arnaud-Vanneau, Erba, Fenner, Head, Pearson, Premoli Silva, Watkins
Paleomagnetism: Gee, Nakanishi
Sedimentation Rates: Arnaud-Vanneau, Erba, Fenner, Head, Pearson, Premoli Silva, Watkins
Inorganic Geochemistry: Opdyke, Wilson
Organic Geochemistry: Buchardt
Igneous Petrology: Christie, Dieu
Physical Properties: Bohrmann, Hobbs, Rack
Downhole Measurements and Seismic Stratigraphy: Bergersen, Ito, Ladd, Larson, Ogg
Summary and Conclusions: Haggerty, Premoli Silva

Following the text of each site chapter are summary core descriptions ("barrel sheets" and basement rock visual core descriptions) and photographs of each core.

Survey and Drilling Data

Geophysical survey data collected during Leg 144 consists of magnetic, bathymetric, and seismic data acquired during the transects from Majuro to Limalok (Harrie) Guyot, from Limalok to Lo-En Guyot, from Lo-En to Wodejebato (Sylvania) Guyot, from Wodejebato to Site 801, from Site 801 to MIT Guyot, and from MIT to Seiko Guyot, as well as data collected between sites. These

are discussed in the "Underway Geophysics" chapter (this volume), along with a brief description of all geophysical instrumentation and acquisition systems used, and a summary listing of Leg 144 navigation. The survey data used for final site selection, including data collected during site surveys before Leg 144 and on short site location surveys during Leg 144, are presented in the "Underway and Site Geophysics" sections of the individual site chapters (this volume). During the Leg 144 *JOIDES Resolution* surveys, single-channel seismic, 3.5- and 12-kHz echo sounder, and magnetic data were recorded across the planned drilling sites to aid in site confirmation before dropping the beacon.

The single-channel seismic profiling system used either two 80-in.³ water guns or a 200-in.³ water gun as the energy source and a Teledyne streamer with a 100-m-long active section. At several sites, one or two 200-in.³ guns were used as sources for sonobuoy seismic refraction shooting. All seismic data were recorded digitally on tape using a Masscomp 561 super minicomputer and were also displayed in real time in analog format on Raytheon electrostatic recorders using a variety of filter settings and scales.

Bathymetric data collected using the 3.5- and 12-kHz precision depth recorder (PDR) system were each displayed on Raytheon recorders. The depths were calculated on the basis of an assumed 1500 m/s sound velocity in water. The water depth (in meters) at each site was corrected for (1) the variation in sound velocity with depth using Matthews's (1939) tables, and (2) the depth of the transducer pod (6.8 m) below sea level. In addition, depths referred to the drilling-platform level are corrected for the height of the rig floor above the water line, which gradually increased throughout the cruise (see Fig. 1).

Magnetic data were first collected using a Geometrics 801 proton precession magnetometer, then displayed on a strip chart recorder, and finally recorded on magnetic tape for later processing.

Drilling Characteristics

Because water circulation downhole is open, cuttings are lost onto the seafloor and cannot be examined. The only available information about sedimentary stratification in uncored or unrecovered intervals, other than from seismic data or wireline logging results, is from an examination of the behavior of the drill string as observed and recorded on the drilling platform. Typically, the harder a layer, the slower and more difficult it is to penetrate. A number of other factors may determine the rate of penetration, so it is not always possible to relate the drilling time directly to the hardness of the layers. Bit weight and revolutions per minute, recorded on the drilling recorder, also influence the penetration rate.

Drilling Deformation

When cores are split, many show signs of significant sediment disturbance, including the downward-concave appearance of originally horizontal bands, haphazard mixing of lumps of different lithologies (mainly at the tops of cores), and the near-fluid state of some sediments recovered from tens to hundreds of meters below the seafloor. Core deformation probably occurs during

¹ Premoli Silva, I., Haggerty, J., Rack, F., et al., 1993. *Proc. ODP, Init. Repts.*, 144; College Station, TX (Ocean Drilling Program).

² Shipboard Scientific Party is as given in the list of participants preceding the contents.

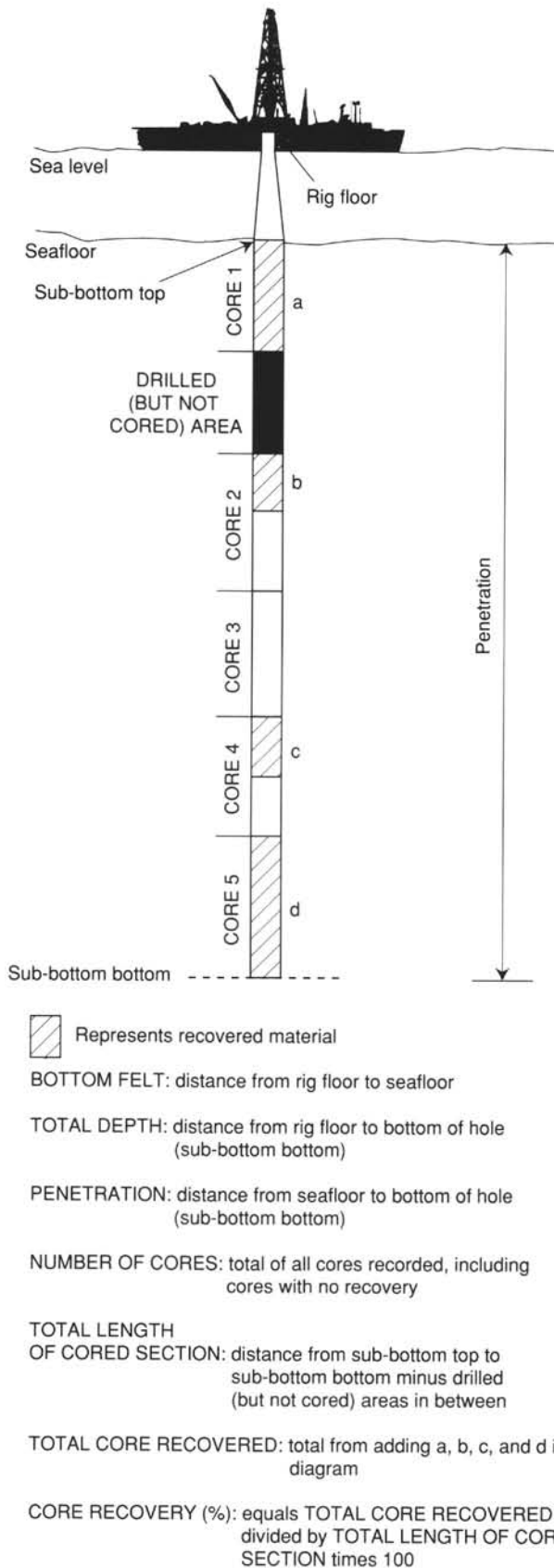


Figure 1. Diagram illustrating terms used in the discussion of coring operations and core recovery.

cutting, retrieval (with accompanying changes in pressure and temperature), and core handling on deck.

Shipboard Scientific Procedures

Numbering of Sites, Holes, Cores, and Samples

Drilling sites are numbered consecutively from the first site drilled by the *Glomar Challenger* in 1968. A site number refers to one or more holes drilled while the ship was positioned over one acoustic beacon. Multiple holes may be drilled at a single site by pulling the drill pipe above the seafloor (out of the hole), moving the ship some distance from the previous hole, and then drilling another hole. In some cases, the ship may return to a previously occupied site to drill additional holes.

For all ODP drill sites, a letter suffix distinguishes each hole drilled at the same site. For example, the first hole drilled is assigned the site number and suffix "A"; the second hole takes the site number and suffix "B"; and so forth. Note that this procedure differs slightly from that used by DSDP (Sites 1 through 624), but this prevents ambiguity between site- and hole-number designations. For sampling purposes, it is important to distinguish among holes drilled at a site. Sediments or rocks recovered from different holes usually do not come from equivalent positions in the stratigraphic column, even if the core numbers are identical.

The cored interval is measured in meters below seafloor (mbsf); sub-bottom depths are determined by subtracting the drill-pipe measurement (DPM) water depth (the length of pipe from the rig floor to the seafloor) from the total DPM (from the rig floor to the bottom of the hole; see Fig. 1). Note that although the echo-sounding data (from the PDRs) are used to locate the site, they are not used as a basis for any further measurements.

The depth interval assigned to an individual core begins with the depth below the seafloor that the coring operation began and extends to the depth that the coring operation ended for that core (see Fig. 1). For rotary coring using the rotary core barrel (RCB) or the extended core barrel (XCB), each coring interval is equal to the length of the joint of drill pipe added for that interval (though a shorter core may be attempted in special instances). The drill pipe in use varies from about 9.4 to 9.8 m. The pipe is measured as it is added to the drill string, and the cored interval is recorded as the length of the pipe joint to the nearest 0.1 m. For advanced hydraulic piston coring (APC) operations, the drill string is advanced 9.5 m, the maximum length of the piston stroke.

Coring intervals are not necessarily adjacent but may be separated by drilled intervals. In soft sediments, the drill string can be "washed ahead" with the core barrel in place, without recovering sediments. This is achieved by pumping water down the pipe at high pressure to wash the sediment out of the way of the bit and up the annulus between the drill pipe and the wall of the hole. If thin, hard, rock layers are present, then it is possible to get "spotty" sampling of these resistant layers within the washed interval and thus to have a cored interval greater than 9.5 m. When drilling hard rock, a center bit may replace the core barrel if it is necessary to drill without core recovery.

Cores taken from a hole are numbered serially from the top of the hole downward. Core numbers and their associated cored intervals in meters below seafloor usually are unique in a given hole; however, this may not be true if an interval must be cored twice because of the caving of cuttings or other hole problems. Maximum full recovery for a single core is 9.5 m of rock or sediment contained in a plastic liner (6.6-cm internal diameter) plus about 0.2 m (without a plastic liner) in the core catcher (Fig. 2). The core catcher is a device at the bottom of the core barrel that prevents the core from sliding out when the barrel is being retrieved from the hole. For sediments, the core-catcher sample is extruded into a short piece of plastic liner and is treated as a

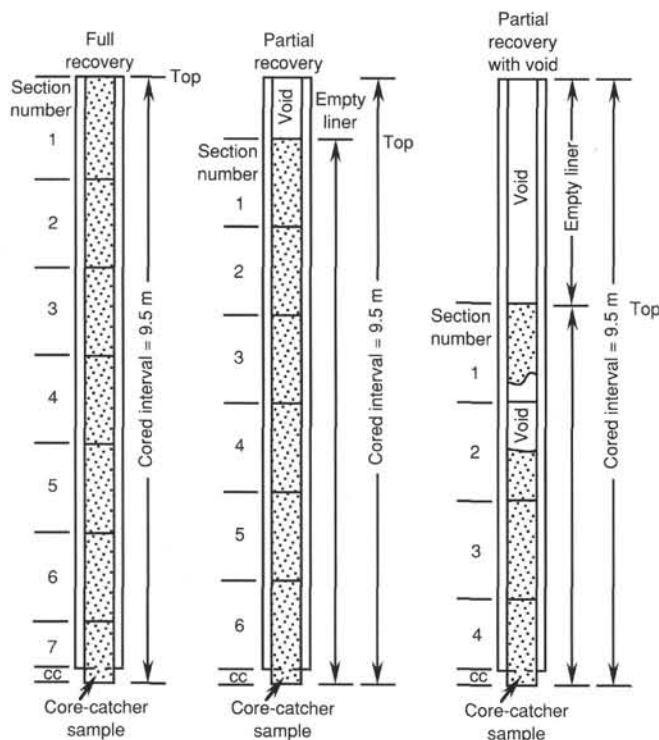


Figure 2. Diagram illustrating procedures used in cutting and labeling core sections.

separate section below the last core section. For hard rocks, material recovered in the core catcher is included at the bottom of the last section. In certain situations (e.g., when coring gas-charged sediments that expand while being brought on deck), recovery may exceed the 9.5-m maximum.

A recovered core is divided into 1.5-m sections that are numbered serially from the top (Fig. 2). When full recovery is obtained, the sections are numbered from 1 through 7, with the last section possibly being shorter than 1.5 m (rarely, an unusually long core may require more than seven sections). When less than full recovery is obtained, as many sections as are needed to accommodate the length of the core will be recovered; for example, 4 m of core would be divided into two 1.5-m sections and one 1-m section. If cores are fragmented (recovery less than 100%), sections are numbered serially and intervening sections are noted as void, whether the shipboard scientists think that the fragments were contiguous in situ or not. In rare cases, a section less than 1.5 m may be cut to preserve features of interest (e.g., lithologic contacts).

By convention, material recovered from the core catcher is placed below the last section when the core is described and is labeled core catcher (CC); in sedimentary cores, it is treated as a separate section. The core catcher is placed at the top of the cored interval in cases where material is recovered only in the core catcher. Information supplied by the drillers or by other sources may allow for more precise interpretation as to the correct position of core-catcher material within an incompletely recovered cored interval.

Igneous or metamorphic rock cores are also cut into 1.5-m sections, which are numbered serially; individual pieces of rock are then each assigned a number. Fragments of a single piece are assigned a single number, and individual fragments are identified alphabetically. The core-catcher sample is placed at the bottom of the last section and is treated as part of the last section, rather than

separately. Scientists completing visual core descriptions describe each lithologic unit, noting core and section boundaries only as physical reference points.

When, as is usually the case, the recovered core is shorter than the cored interval, the top of the core is equated with the top of the cored interval by convention, to achieve consistency in handling analytical data derived from the cores. Samples removed from the cores are designated by distance measured in centimeters from the top of the section to the top and bottom of each sample removed from that section. In curated hard-rock sections, sturdy plastic spacers are placed between pieces that did not fit together to protect them from damage in transit and in storage. Therefore, the centimeter interval noted for a hard-rock sample has no direct relationship to that sample's depth within the cored interval; it is only a physical reference to the location of the sample within the curated core.

A complete identification number for a sample consists of the following information: leg, site, hole, core number, core type, section number, piece number (for hard rock), and interval in centimeters measured from the top of section. For example, a sample identification of "144-871C-5R-1, 10-12 cm," would be interpreted as representing a sample removed from the interval between 10 and 12 cm below the top of Section 1, Core 5 ("R" designates that this core was taken during rotary coring) of Hole 871A during Leg 144.

All ODP core and sample identifiers indicate core type. The following abbreviations are used: R = rotary core barrel (RCB); H = hydraulic piston core (HPC; also referred to as APC, or advanced hydraulic piston core); P = pressure core sample; X = extended core barrel (XCB); B = drill-bit recovery; C = center-bit recovery; I = in-situ water sample; S = sidewall sample; W = wash-core recovery; V = vibrapercussive core (VPC); N = motor-driven core barrel (MDCB), and M = diamond core barrel (DCB). Numerous coring systems were used on Leg 144. These include APC, XCB, MDCB, DCB, standard RCB, and the "anti-whirl" polycrystalline diamond compact (PDC) drag-type bit as an alternative technology for RCB coring in sedimentary rocks.

Core Handling

Sediments

As soon as a core is retrieved on deck, a sample is taken from the core catcher and given to the paleontological laboratory for an initial age assessment. The core is then placed on the long horizontal rack, and gas samples may be taken by piercing the core liner and withdrawing gas into a vacuum tube. Voids within the core are sought as sites for gas sampling. Some of the gas samples are stored for shore-based study, but others are analyzed immediately as part of the shipboard safety and pollution-prevention program. Next, the core is marked into section lengths, each section is labeled, and the core is cut into sections. Interstitial water (IW) and whole-round samples are then taken. In addition, some headspace gas samples are scraped from the ends of cut sections on the catwalk and sealed in glass vials for light hydrocarbon analysis. Each section is then sealed at the top and bottom by gluing on color-coded plastic caps, blue to identify the top of a section and clear for the bottom. A yellow cap is placed on the section ends from which a whole-round sample has been removed, and the sample code (e.g., interstitial water [IW] or physical properties [PP]) is written on the yellow cap. The caps are generally attached to the liner by coating the end liner and the inside rim of the cap with acetone and then taping the caps to the liners.

Afterward, the cores are carried into the laboratory, where the sections are again labeled, using an engraver to mark the complete designation of the section permanently. The length of the core in each section and the core-catcher sample are measured to the

nearest centimeter; this information is logged into the shipboard CORELOG data-base program.

Whole-round sections from APC and XCB cores are normally run through the multisensor track (MST). The MST includes the gamma-ray attenuation porosity evaluator (GRAPE) and *P*-wave logger (PWL) devices, which measure bulk density, porosity, and sonic velocity; it also includes a sensor that determines the volume magnetic susceptibility. Relatively soft sedimentary cores are equilibrated to room temperature (by waiting approximately 3 hr) if thermal conductivity measurements are to be performed on them.

Cores of soft material are split lengthwise into working and archive halves. The softer cores are split with a wire or saw, depending on the degree of induration. The wire-cut cores are split from the bottom to top, so investigators need to be aware that older material could have been transported up the core on the split face of each section. In well-lithified sediment cores, the core liner is split and the top half removed so that the whole-round core can be observed before choosing whole-round samples for and macro-fossil paleontology. Lithified cores are then split with a band saw or diamond saw.

The working half of the core is sampled for both shipboard and shore-based laboratory studies. Each extracted sample is logged into the sampling computer data-base program by their location in the core and the name of the investigator receiving the sample. Records of all of the samples removed are kept by the curator at ODP headquarters. The extracted samples are sealed in plastic vials or bags and labeled. Samples are routinely taken for shipboard physical-properties analysis. These samples are subsequently used after drying, to provide coulometric analysis for calcium carbonate and CNS elemental analysis for organic carbon; these data are reported in the site chapters.

The archive half of the core is described visually. Smear slides of soft sediment are made from samples taken from the archive half, these are supplemented by thin sections (of both soft sediments and hard rocks) taken from the working half. Smear slide and thin section descriptions are entered into the SLIDES data base, and the smear slides and thin sections are curated at the Gulf Coast Repository at the Ocean Drilling Program. Most archive sections are run through the cryogenic magnetometer. The archive half is then photographed with both black-and-white and color film, a whole core at a time. Close-up photographs (black-and-white) are taken of particular features for illustrations in the summary of each site, as requested by individual scientists.

Both halves of the core are placed into labeled plastic tubes, sealed, and transferred to cold-storage space aboard the drilling vessel. Leg 144 cores were transferred from the ship in refrigerated air freight containers to cold storage at the Gulf Coast Repository of the Ocean Drilling Program, Texas A&M University, College Station, Texas.

Igneous and Metamorphic Rocks

Igneous and metamorphic rock cores are handled differently from sedimentary cores. Once on deck, the core catcher is placed at the bottom of the core liner, and total core recovery is calculated by shunting the rock pieces together and measuring to the nearest centimeter; this information is logged into the shipboard core-log data-base program. The core is then cut into 1.5-m-long sections and transferred into the lab.

The contents of each section are transferred into 1.5-m-long sections of split core liner, where the bottoms of oriented pieces (i.e., pieces that clearly could not have rotated top to bottom about a horizontal axis in the liner) are marked with a red wax pencil. This is to ensure that orientation is not lost during the splitting and labeling process. Important primary features of the cores are also recorded at this time. The core is then split into archive and

working halves using a diamond saw blade. Plastic spaces are used to separate individual pieces and/or reconstructed groups of pieces in the core liner. These spacers may represent a substantial interval of no recovery. Pieces are numbered sequentially from the top of each section, beginning with piece number 1; reconstructed groups of pieces are assigned the same number but are lettered consecutively. Pieces are labeled only on external surfaces. If the piece is oriented, an arrow is added to the label pointing to the top of the section. Normally, as pieces are free to turn about a vertical axis during drilling, azimuthal orientation of a core is not possible.

In splitting the core, every effort is made to ensure that important features are represented in both halves. The working half is sampled for shipboard physical properties measurement, magnetic studies, X-ray fluorescence (XRF), X-ray diffraction (XRD), and thin-section studies. Nondestructive physical properties measurements, such as magnetic susceptibility, are made on the archive half of the core. Where recovery permits, samples are taken from each lithologic unit. Some of these samples are mini-cores.

The working half of the hard-rock core is then sampled for shipboard laboratory studies. Records of all samples are kept by the curator at ODP.

The archive half of the core is described visually, then photographed with both black-and-white and color film, one core at a time. Both halves of the core are then shrink-wrapped in plastic to prevent rock pieces from vibrating out of sequence during transit, put into labeled plastic tubes, sealed, and transferred to cold-storage space aboard the drilling vessel. As with the other Leg 144 cores, they are housed at the Gulf Coast Repository.

VISUAL CORE DESCRIPTIONS OF SEDIMENTS

Core Description Forms and the "VCD" Program

The core description forms (Fig. 3), or "barrel sheets," summarize the data obtained during shipboard analysis of each sediment core. On Leg 144, these were generated using the ODP in-house Macintosh application "VCD" (edition 1.0.1, §12, customized for this leg). The following discussion explains the ODP conventions used in compiling each part of the core description forms, the use of "VCD" to generate these forms, and the exceptions and additions to these procedures adopted by the Leg 144 Shipboard Scientific Party. Many departures from ODP conventions, especially those related to the description of shallow-water carbonates, are based on the experiences of the Leg 143 Shipboard Scientific Party, who also drilled Pacific guyots.

Shipboard sedimentologists were responsible for visual core description, smear-slide analyses, and thin-section descriptions of sedimentary material. Core descriptions were initially recorded by hand on a section-by-section basis on standard ODP visual core description forms (VCD forms, not to be confused with the "VCD" Macintosh application). On some recent ODP legs, visual description was conducted directly at the core-by-core level using the computerized VCD application. On Leg 144, however, we considered that it was desirable to preserve observations of fine detail that are lost at the core-by-core "barrel sheet" level. Copies of the original visual core description forms are available from ODP on request.

Hand-drawn "barrel sheets," used by ODP up through Leg 135, included columns for information on biostratigraphic zonations, geochemistry (CaCO₃, C_{org}, XRF), paleomagnetism, and physical properties (wet-bulk density and porosity). Much of this information is somewhat redundant at the core-by-core level. Core description forms generated directly by the VCD Macintosh application comprise a condensed version of the information normally recorded on the section-by-section visual core description sheets,

SITE 871 HOLE A CORE 1H

CORED 0.0 - 9.5 mbsf

Meter	Graphic lithology	Section	Age	Structure	Disturb.	Sample	Color	Description
1		1						
2		2						
3		3						
4		4						
5		5						
6		6						
7								
8								
9								

Figure 3. Core description form ("barrel sheet") used for sediments and sedimentary rocks.

supplemented only by a column indicating age. However, the VCD application offers an alternate representation of the core description forms as a PICT file, allowing their manipulation by Macintosh graphics applications. By this means, it is possible to attach columns with additional graphics or text information (e.g., biostratigraphy, magnetostratigraphy, chemical data, GRAPE data, and magnetic susceptibility) where useful. For Leg 144, we created an additional form that illustrated expanded biostratigraphic information (see Fig. 4). Customization of the VCD application allowed the addition of sedimentary structures, graphic lithologies, and other features specific to this leg.

Core Designation

Cores are designated using leg, site, hole, core number, and core type as discussed in a preceding section (see "Numbering of Sites, Holes, Cores, and Samples" section, this chapter). The cored interval is specified in terms of meters below sea level (mbsl) and meters below seafloor (mbsf). On the basis of drill-pipe measurements (DPM), reported by the SEDCO coring technician and the ODP operations superintendent, depths are corrected for the height of the rig-floor dual elevator stool above sea level to give true water depth and correct mbsl.

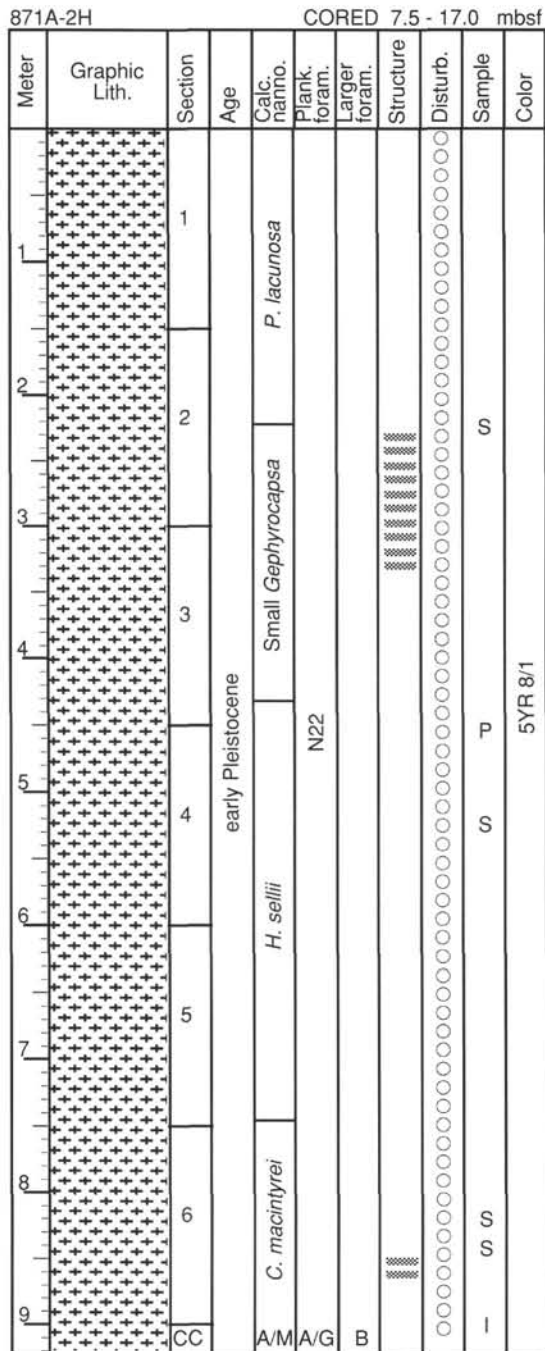


Figure 4. Sample of a core description form with additional biostratigraphic information.

Graphic Lithology Column

The lithology of the recovered material is represented on the core description forms by as many as three symbols in the column titled "Graphic Lithology" (Fig. 5). Where an interval of sediment or sedimentary rock is a homogeneous mixture, the constituent categories are separated by a solid vertical line, with each category represented by its own symbol. Constituents accounting for <10% of the sediment in a given lithology (or others remaining after the representation of the three most abundant lithologies) are

not shown in the graphic lithology column but are listed in the "Lithologic Description" section of the core description form. In an interval comprising two or more sediment lithologies that have quite different compositions, such as in thin-bedded and highly variegated sediments, the average relative abundances of the lithologic constituents are represented graphically by dashed lines that vertically divide the interval into appropriate fractions, as described above. The graphic lithology column can display only the composition of layers or intervals exceeding 20 cm in thickness. Because the VCD application does not allow scale expansion, the graphic lithology is generally not legible when core recovery is 20 cm; therefore, important lithologic information is contained in the "Lithologic Description" section.

Age Column

The chronostratigraphic unit, as recognized on the basis of paleontologic and paleomagnetic data, is shown in the column entitled "Age" on the core description forms. Boundaries between assigned ages are indicated as follows:

1. Sharp boundary: horizontal line;
2. Unconformity or hiatus: horizontal line with + signs above it; and
3. Uncertain: horizontal line with question marks.

Biostratigraphy

The VCD application does not permit addition of biostratigraphic zones and fossil abundances typically included in barrel sheets prior to Leg 138. We modified the VCD barrel sheets post-cruise to include columns for calcareous nannofossil zones and abundance, planktonic foraminifer zones and abundance, and larger foraminifer abundance.

Sedimentary Structures and Components

In sediment cores, natural structures and structures created by the coring process can be difficult to distinguish. Natural structures observed in the cores are indicated in the "Structure and Components" column of the core description forms. Sedimentary components are not typically annotated on the visual core description form, although for Legs 143 and 144 sedimentary components, particularly of platform carbonates such as ooids, algae, bryozoans, etc., were indicated in the "Structure and Components" column by custom symbols when space permitted. The column is divided into three vertical areas for symbols (Fig. 6). Because of limited space in the core description forms, only a few important sedimentary structures and components can be represented. A more complete summary of structures and constituents may be found in the "Lithologic Description" column.

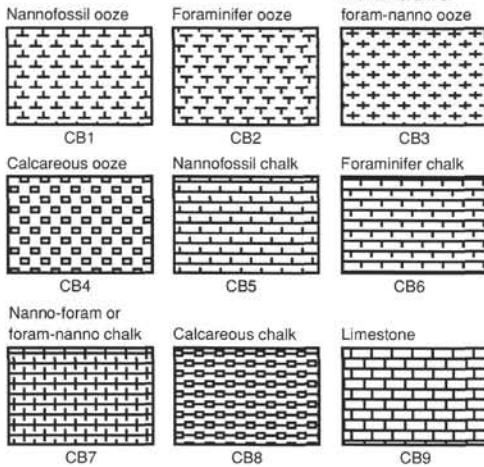
Sediment Disturbance

Sediment disturbance resulting from the coring process is illustrated in the "Disturbance" column on the core description forms (using symbols in Fig. 6) when space permits. Blank regions indicate a lack of drilling disturbance. The degree of drilling disturbance is described for soft and firm sediments using the following categories:

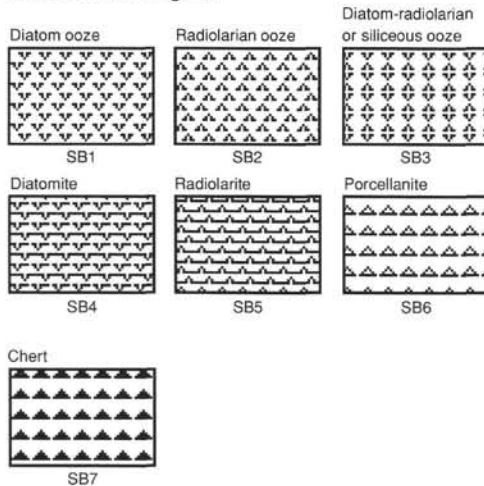
1. Slightly deformed: bedding contacts are slightly bent;
2. Moderately deformed: bedding contacts have extreme bowing;
3. Highly deformed: bedding is completely disturbed, in some places showing apparent diapir or flow structures; and
4. Soupy: intervals are water saturated and have lost all aspects of original bedding.

Biogenic pelagic sediments

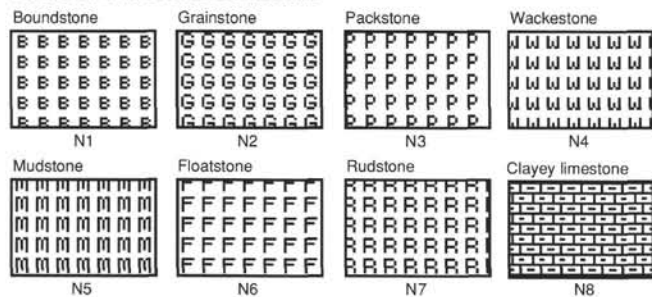
Calcareous lithologies



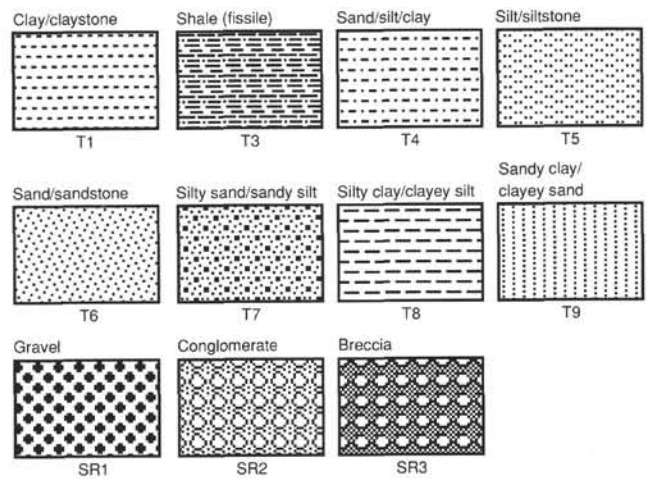
Siliceous lithologies



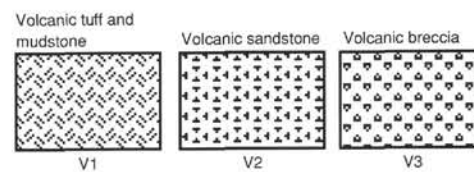
Platform carbonate sediments



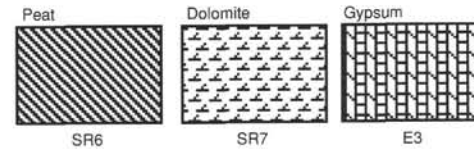
Siliciclastic sediments and rocks



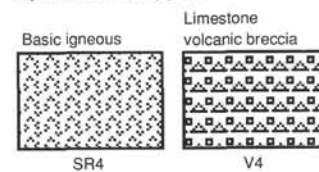
Volcaniclastic sediments and rocks



Chemical sediments or rocks



Special rock types



Mixed sediments

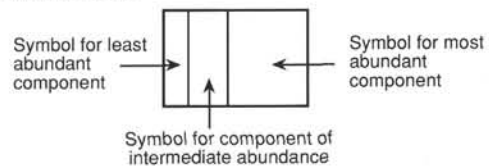


Figure 5. Key to symbols used in the “graphic lithology” column on the core description form shown in Figure 3.

On Leg 144, we adopted a drilling disturbance scale for platform limestones to evaluate the reliability of the apparent stratigraphic sequence, especially in rotary-drilled cores with low recovery. The uppermost rocks in a rotary core may be suspect as caved boulders, cobbles, or gravels if: (1) the lithology is a repetition of an overlying interval, (2) the biostratigraphic age is out of sequence, or (3) the lithofacies continuity is disrupted.

We defined a three-unit scale of “drilling disturbance” that is based on the terms: cylinders (CY), rollers (RL), and drilling pebbles (DP). We felt that this scale is more objective and yields more useful information in these deposits than the terms recommended in the

ODP Handbook for Shipboard Sedimentologists (Mazzullo and Graham, 1988). Our new terms are defined as follows:

1. *Cylinders (CY)*: pieces of core that are too long to have rotated end over end within the core barrel, even though the corners may be rounded.

2. *Rollers (RL)*: rounded fragments that could have rotated end over end within the core barrel, but are too large to have moved past adjacent fragments.

3. *Drilling pebbles (DP)*: fragments of any shape that could have slipped past adjacent fragments.

Drilling disturbance symbols

Soft Sediments

	Slightly disturbed
	Moderately disturbed
	Highly disturbed
	Soupy
<u>Hard sediments</u>	
	Slightly fractured
	Moderately fractured
	Highly fractured
	Drilling breccia

Sedimentary components and structures

	Red algae		Coated grain
	Green algae		Vugs
	Blue-green algae (cyanobacteria)		Keystone vugs
	Benthic foraminifers		Bird's-eye vugs
	Planktonic foraminifers		Hardground
	Serpulids		Dolomite
	Rudist bivalves		Glauconite
	Other bivalves		Phosphorite
	Gastropods		Manganese
	Hermatypic corals		Pyrite
	Solitary corals		Chert
	Echinoderms		Lithoclast
	Bryozoan		Bioturbation, minor
	Plant debris		Bioturbation, moderate
	Shell fragments		Bioturbation, strong
	Pellets		Planar laminae
	Peloids		Wavy laminae
	Ooids		Cross-laminae
	Oncoids		Upward-fining sequence
			Desiccation crack

Figure 6. Symbols used for drilling disturbance and sedimentary structures and components on core description forms shown in Figure 3.

All pieces were inspected for orientation of geopetal structures, for fitting of end surfaces with adjacent fragments and for lithofacies continuity. The distinction between cylinders and rollers was determined from an examination of the archive half of the split core. The scale of the core description forms generated by the VCD application does not permit representation of this drilling disturbance scheme on a piece-by-piece basis, therefore, this information is summarized under the heading of "General Description" in the "Lithologic Description" column of the computer generated visual core description form.

The degree of fracturing in lithified sediment is described using the following categories:

1. Slightly fractured: core pieces are in place and contain little drilling slurry or breccia;
2. Moderately fragmented: core pieces are in place or partly displaced, but original orientation is preserved or recognizable (drilling slurry may surround fragments);
3. Highly fragmented: pieces are from the interval cored and probably in correct stratigraphic sequence (although they may not represent the entire section), but original orientation is completely lost;
4. Drilling breccia: core pieces have lost their original orientation and stratigraphic position and may be mixed with drilling slurry.

Color

The hue and chroma attributes of color were determined by comparison with Munsell soil-color charts (Munsell Soil Color Charts, 1971). This was done as soon as possible after the cores were split because redox-associated color changes may occur when deep-sea sediments are exposed to the atmosphere. Information on sediment colors is given in the "Color" column on the core description forms.

Samples

The position and type of samples taken from each core for shipboard analysis is indicated in the "Samples" column on the core description form, as follows:

- S: smear slide,
- T: thin section,
- P: physical properties sample,
- M: micropaleontology sample,
- X: paleomagnetic sample,
- I: interstitial water sample,
- C: organic geochemistry sample,
- D: XRD sample,
- F: XRF sample, and
- A: acetate peels.

When recovery is <20 cm in a core, sample locations are listed by section and interval in the "Lithologic Description."

Lithologic Description—Text

The lithologic description that appears on each core description form consists of three parts: (1) a heading that lists all the major sediment lithologies observed in the core (see "Sedimentary Petrology" section, this chapter); (2) a more detailed description of these sediments, including features such as color, composition (determined from the analysis of smear slides), sedimentary structures, or other notable characteristics (descriptions and locations of thin, interbedded, or minor lithologies that cannot be depicted in the graphic lithology column are included under this heading); and (3) for limestones, a list of cylinders, rollers and drilling pebbles.

Smear Slide and Thin Section Summary

Where appropriate, a figure summarizing data from smear slides and thin sections appears in each site chapter. A table summarizing data from smear slides and thin sections appears at the end of each site chapter. The table includes information on the sample location, whether the sample represents a dominant ("D") or minor ("M") lithology in the core, and the estimated percentages of sand-, silt-, and clay-size material, together with all identified components. In many cored intervals, the lithology is highly variable on scales of 10 cm to 10 m.

SEDIMENTARY PETROLOGY

The different core lithologies drilled during Leg 144 were described based upon a modified sediment classification scheme proposed by the Ocean Drilling Program (Mazzullo et al., 1988). The Leg 144 classification has kept the two basic sediment and rock types described in Mazzullo et al. (1988) as *granular* and *chemical* sediments and rocks.

As shown in Table 1 (Mazzullo and Graham, 1988), granular sediments and rocks were subdivided in two lithologic groups: *calcareous* and *siliceous*. The calcareous and siliceous lithologies were each separated into two classes: *pelagic* and *nonpelagic*. The calcareous nonpelagic lithologies are largely constituted by particles generated in shallow water. The siliceous nonpelagic class is divided into two subclasses: *siliciclastics* and *volcaniclastics*.

Classes of Granular Sediments and Rocks

The definitions of pelagic and nonpelagic grain types that occur in granular sediments are as follows:

Pelagic grains are fine-grained skeletal debris produced within the upper part of the water column in open-marine environments by

1. calcareous microfauna (e.g., foraminifers, pteropods), microf flora (e.g., nannofossils), and associated organisms; and
2. siliceous microfauna (radiolarians), microf flora (diatoms), and associated organisms (sponge spicules, a common benthic component of siliceous oozes, are included for convenience).

Nonpelagic grains are coarse- to fine-grained particles deposited in hemipelagic and near-shore environments, such as

1. calcareous skeletal and nonskeletal grains and fragments (e.g., bioclasts, peloids, calcareous mud) (note that the term *calcareous mud* is used to define very fine calcareous particles (<20 μm) with no clear identification of origin observed in smear slides; they can be either recrystallized nannofossils or nonpelagic, platform derived calcareous mud in pelagic lithologies);
2. siliciclastic grains comprising minerals and rock fragments that were eroded from plutonic, sedimentary, and metamorphic rocks; and
3. volcaniclastic grains comprising glass shards, rock fragments, and mineral crystals that were produced by volcanic processes and include epiclastic sediments (eroded from volcanic rocks by wind, water, or ice), pyroclastic sediments (products of explosive magma degassing), and hydroclastic sediments (granulation of volcanic glass by steam explosions).

Variations in the relative proportions of these five grain types define five major classes of granular sediments and rocks (Fig. 7):

1. *Pelagic* sediments and rocks contain more than 60% pelagic and neritic grains and fewer than 40% siliciclastic and volcaniclastic grains, as well as a higher proportion of pelagic than neritic grains.

Table 1. Outline of the granular sediment classification scheme used on Leg 144.

I. Granular sediments and rocks	
A. Calcareous lithologies	
1. Pelagic sediments and rocks	
Ooze:	
Nannofossil ooze	- CB1
Foraminifer ooze	- CB2
Nannofossil foraminifer ooze or foraminifer nannofossil ooze	- CB3
Calcareous ooze	- CB4
Chalk:	
Nannofossil chalk	- CB5
Foraminifer chalk	- CB6
Nannofossil foraminifer chalk or foraminifer nannofossil chalk	- CB7
Calcareous chalk	- CB8
Limestone:	
Limestone	- CB9
2. Nonpelagic sediments and rocks (modified for degree of firmness:	
U = unlithified, and PL = partially lithified)	
Boundstone	- N1
Grainstone	- N2 (UGR, PLGR, GR)
Packstone	- N3 (UPK, PLPK, PK)
Wackestone	- N4 (UWK, PLWK, WK)
Mudstone	- N5 (UN5, PLN5)
Floatstone	- N6 (UFT, PLFT, LFT)
Rudstone	- N7 (ULRD, PLRD, LRD)
Clayey limestone	- N8
B. Siliceous lithologies	
1. Pelagic sediments and rocks	
Diatom ooze	- SB1
Radiolarian ooze	- SB2
Diatom-radiolarian or siliceous ooze	- SB3
Diatomite	- SB4
Radiolarite	- SB5
Porcellanite	- SB6
Chert	- SB7
2. Nonpelagic sediments and rocks	
Siliciclastic sediments and rocks	
Clay	- T1
Shale (fissile)	- T3
Sand/silt/clay	- T4
Silt	- T5
Sand	- T6
Silty sand/sandy silt	- T7
Silty clay/clayey silt	- T8
Sandy clay/clayey sand	- T9
Gravel	- SR1
Conglomerate	- SR2
Breccia	- SR3
Volcaniclastic sediments and rocks	
Volcanic tuff and mudstone	- V1
Volcanic sandstone	- V2
Volcanic breccia	- V3
Special rock types	
Basic igneous	- SR4
Limestone volcanic breccia	- V4
II. Chemical sediments or rocks	
A. Carbonaceous sediments and rocks	
Peat	- SR6
B. Evaporites	
Gypsum	- E3
C. Silicates	
Porcellanite	- SB6
Chert	- SB7
D. Carbonates	
Dolomite	- SR7

2. *Neritic* sediments and rocks are composed of more than 60% pelagic and neritic grains and fewer than 40% siliciclastic and volcaniclastic grains; they also contain a higher proportion of neritic than pelagic grains.

3. *Siliciclastic* sediments and rocks are composed of more than 60% siliciclastic and volcaniclastic grains and fewer than 40% pelagic and neritic grains; they also contain a higher proportion of siliciclastic than volcaniclastic grains.

4. *Volcaniclastic* sediments and rocks are composed of more than 60% siliciclastic and volcaniclastic grains and fewer than 40% pelagic and neritic grains; also, a higher proportion of volcaniclastic than siliciclastic grains are present.

5. *Mixed* sediments and rocks are composed of 40% to 60% siliciclastic and volcaniclastic grains, and 40% to 60% pelagic and neritic grains. Appropriate modifiers are used to note major components.

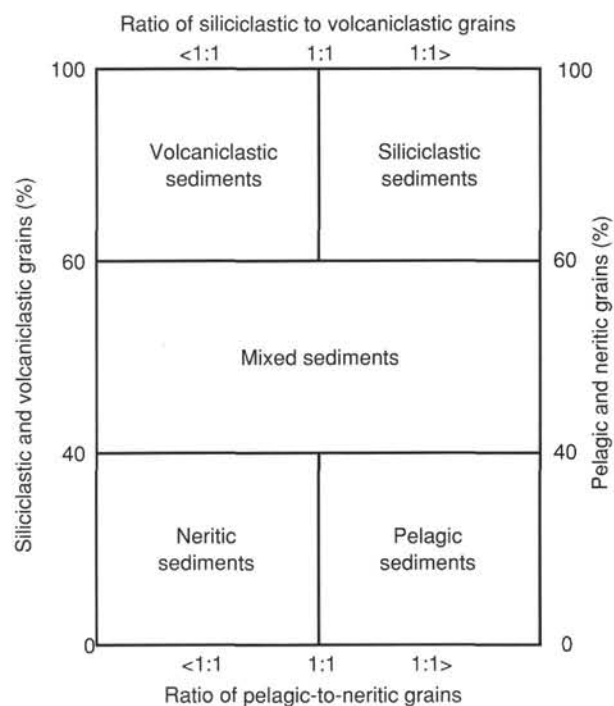


Figure 7. Diagram illustrating classes of granular sediments (from Mazzullo and Graham, 1988, p. 47).

Methods of Description

Composition and Texture

Sediment and rock names were defined solely on the basis of composition and texture. Composition defines the name for those deposits more characteristic of open-marine (pelagic) conditions. Textural names and compositional modifiers are used for hemipelagic and near-shore (nonpelagic) facies. Data on composition and texture of cored sediments and rocks were primarily determined aboard ship by visual observation of core, smear slides, thin sections, acetate peels, and coarse fractions with the aids of hand lens and microscope. Calcium carbonate content was qualitatively estimated in smear slides and quantitatively measured using coulometer analyses of inorganic carbon (see "Organic Geochemistry" section, this chapter). Qualitative evaluations of mineral composition of indurated nonpelagic limestones were obtained by staining of selected samples with alizarin-red S following the methods outlined in Lewis (1984).

X-ray Diffraction Analyses

A Philips ADP 3720 X-ray diffractometer was used for the X-ray diffraction (XRD) analysis of mineral phases. $\text{CuK}\alpha$ radiation was measured through a Ni filter at 40 kV and 35 mA. The goniometer scanned from 2° to 70° 2θ with a step size of 0.01° , and the counting time was 0.5 per step.

Samples were ground in steel containers in a Spex 8000 Mixer Mill or with an agate pestle and mortar. The powder was then pressed into the sample holders or mixed with water, placed on glass slides with a pipet, and dried. The glass slides were then mounted with parafilm into sample holders for analysis.

Firmness

The determination of induration is highly subjective, and the categories used on Leg 144 (after Gealy et al., 1971) are thought

to be practical and significant. Three classes of firmness for calcareous sediments and rocks were recognized:

1. *Unlithified*: soft sediments that have little strength and are readily deformed under the pressure of a fingernail or the broad blade of a spatula. This corresponds to the term *ooze* for pelagic calcareous sediments. In nonpelagic calcareous sediments, the prefix *unlithified* is used (e.g., “unlithified packstone”).

2. *Partly lithified*: firm and friable sediments that can be scratched with a fingernail or the edge of a spatula blade. This corresponds to the term *chalk* for pelagic calcareous materials. In nonpelagic calcareous sediment, the prefix *partly lithified* is used (e.g., “partly lithified grainstone”).

3. *Lithified*: hard, nonfriable cemented rock, difficult or impossible to scratch with a fingernail or the edge of a spatula. This corresponds to the term *limestone* (lithified ooze) for pelagic calcareous material. In nonpelagic calcareous material, no prefix is used (e.g., a lithified floatstone is simply called floatstone).

There are only two classes of firmness for *siliceous sediments and rocks*:

1. *Soft*: sediment core can be split with a wire cutter. Soft terrigenous sediment, pelagic clay, and transitional calcareous sediments are termed sand, silt, or clay. For pelagic sediment microfossils, use the names given in the following section.

2. *Hard*: the core is hard (i.e., consolidated or well indurated) if it must be cut with a hand or diamond saw. For these materials, the suffix “-stone” is added to the soft-sediment name (e.g., sandstone, siltstone, and claystone). Note that this varies from terms used to describe nonpelagic calcareous sediments, for which the suffix “-stone” has no firmness implications.

Principal Names

We classified granular sediment during Leg 144 by designating a principal name and major and minor modifiers. The principal name of a granular sediment defines its granular-sediment class; the major and minor modifiers describe the texture, composition, fabric and/or roundness of the grains themselves.

Each granular-sediment class has a unique set of principal names. For pelagic sediments and rocks, the principal name describes the composition and degree of consolidation using the following terms:

1. *Ooze*: unconsolidated calcareous and/or siliceous pelagic sediment;

2. *Chalk*: firm pelagic sediment composed predominantly of calcareous pelagic grains;

3. *Limestone*: hard pelagic sediment composed predominantly of calcareous pelagic grains;

4. *Radiolarite*, *diatomite*, and *spiculite*: firm pelagic sediment composed predominantly of siliceous radiolarians, diatoms, and sponge spicules, respectively;

5. *Porcellanite*: a well-indurated rock with abundant authigenic silica but less hard, lustrous, or brittle than chert (in part, such rocks may represent mixed sedimentary rock);

6. *Chert*: vitreous or lustrous, conchoidally fractured, highly indurated rock composed predominantly of authigenic silica.

The principal name for nonpelagic calcareous sediments and rocks describes the texture and fabric. We use Embry and Klovan's (1971; Fig. 8) amplification of the original Dunham (1962) classification.

Allochthonous limestone: original components not organically bound during deposition, fewer than 10% grains greater than 2 mm in size.

1. *Mudstone*: mud-supported fabric, fewer than 10% grains.

2. *Wackestone*: mud-supported fabric, more than 10% grains.

3. *Packstone*: grain-supported fabric, intergranular mud.

4. *Grainstone*: grain-supported fabric, no intergranular mud.

Floatstone limestone: more than 10% grains greater than 2 mm in size. The matrix (components <2 mm) can be described separately, if appropriate; for example, floatstone, packstone matrix, etc. (Embry and Klovan, 1971).

1. *Floatstone*: matrix-supported fabric.

2. *Rudstone*: grain-supported fabric.

Autochthonous limestone: original components organically bound during deposition (boundstone of Dunham, 1962).

1. *Bafflestone*: formed by organisms that act as baffles;

2. *Bindstone*: formed by organisms that encrust and bind; and

3. *Framestone*: formed by organisms that build a rigid framework.

Crystalline limestone: depositional texture not recognizable (Dunham, 1962).

Chalky limestone: Some of the limestones encountered in Leg 144 were altered into highly porous, “micritic” rock. We describe such limestones informally as *chalky*; for example, “chalky packstone” where the original depositional texture is discernible or “chalky crystalline limestone” where the original texture cannot be recognized.

For siliciclastic sediments, texture provides the main criterion for selection of a principal name. The Udden-Wentworth grain-size scale (Fig. 9) defines the grain-size ranges and the names of the textural groups (*gravel*, *sand*, *silt*, and *clay*) and subgroups (*fine sand*, *coarse silt*, etc.). When two or more textural groups or subgroups are present, the principal names appear in order of increasing abundance. Eight major textural categories can be defined on the basis of relative proportions of sand, silt, and clay (see Table 1). However, in practice, distinctions between some of the categories are dubious without accurate measurements of weight percentages. This is particularly true for the boundary between silty clay and clayey silt. The suffix “-stone” is affixed to the principal names sand, silt, and clay when the sediment is lithified. The terms *conglomerate* and *breccia* are the principal names of gravels with well-rounded and angular clasts, respectively.

For volcaniclastic sediments, the principal name is also dictated by the texture. The classification scheme adopted on Leg 144 does not differentiate between epiclastic, pyroclastic, and hydroclastic volcanics; therefore, we did not find the classification of Fisher and Schmincke (1984) entirely satisfactory as the terms *lapilli* and *ash* have genetic as well as textural connotations. Consequently, we adopted the terms *volcanic sand* and *volcanic sandstone* for sediments and rocks with sand-sized volcaniclastic grains of indeterminate origin. *Volcanic breccia* was used to represent pyroclasts greater than 64 mm in diameter.

In addition, we have found it useful to adopt the term *clayey limestone*, with an appropriate legend, for those limestones containing substantial amounts of clay minerals and which might, in the field, be described as “marly.”

Major and Minor Modifiers

To describe the lithology of the granular sediments and rocks in greater detail the principal name of a granular-sediment class is preceded by major modifiers and followed by minor modifiers. Minor modifiers are preceded by the term *with*. The most common uses of major and minor modifiers are to describe the composition and textures of grain types that are present in major (25%–40%)

Allochthonous limestones: original components not organically bound during deposition					Autochthonous limestones: original components organically bound during deposition				
Fewer than 10% > 2 mm components				More than 10% > 2 mm components		By organisms that act as baffles	By organisms that encrust and bind	By organisms that build a rigid framework	
Contains lime mud (< 0.03 mm)			No lime mud						
Mud supported		Grain supported			Matrix supported				> 2 mm component supported
Fewer than 10% grains (> 0.03 mm < 2 mm)	More than 10% grains								
Mudstone	Wackestone	Packstone	Grainstone	Floatstone	Rudstone	Bafflestone	Bindstone	Framestone	

Figure 8. The Dunham (1962) classification of limestones according to depositional texture, as modified by Embry and Klovan (1971).

and minor (<25%) proportions. In addition, major modifiers can be used to describe grain fabric, grain shape, and sediment color.

The composition of pelagic grains can be described in greater detail with the major and minor modifiers *nannofossil*, *foraminifer*, *calcareous*, *diatom*, *radiolarian*, *spicule*, and *siliceous*. The terms *calcareous* and *siliceous* are used to describe sediments that are composed of calcareous or siliceous pelagic grains of uncertain origin.

The compositional terms for nonpelagic calcareous grains include the following examples of major and minor modifiers as skeletal and nonskeletal grains:

1. *Skeletal*: fragments of varied skeletal material not described in detail;

2. *Ooid*: spherical or elliptical nonskeletal particles smaller than 2 mm in diameter, with or without a central nucleus surrounded by a rim with concentric or radial fabric;

3. *Pisoid* (or *pisolith*): spherical or ellipsoidal nonskeletal particle, commonly greater than 2 mm in diameter, with or without a central nucleus but displaying multiple concentric layers or radial carbonate;

4. *Oncoid* (or *oncolith*): spheroidal stromatolite, displaying multiple concentric layers of carbonate produced by the trapping and binding action of cyanobacteria, distinguished from pisoids by containing sediment and crinkly laminations;

5. *Rhodolith*: spheroidal ball of predominantly coralline algae and other encrusters;

6. *Pellet*: fecal particles from deposit-feeding organisms;

7. *Peloid*: micritic carbonate particle of unknown origin;

8. *Intraclast*: reworked carbonate-sediment/rock fragment or rip-up clast consisting of the same lithology as the host sediment. Degree of lithification should be stated if appropriate.

9. *Lithoclast*: reworked carbonate-sediment/rock fragment consisting of a different lithology than the host sediment. Degree of lithification should be stated if appropriate.

10. *Rudist*: containing abundant rudistid fragments;

11. *Echinoderm*: containing abundant echinoderm fragments;

12. *Algal*: containing abundant algal debris (not to be used for algal stromatolites);

13. *Coralline*: containing abundant coral debris;

14. *Gastropod-rich*: containing abundant gastropod debris;

15. *Molluscan*: containing abundant unspecified molluscan debris.

The textural designations for siliciclastic grains use standard major and minor modifiers such as *gravel(-ly)*, *sand(-y)*, *silt(-y)*, and *clay(-ey)* (Shepard, 1954). The character of siliciclastic grains can be described further by mineralogy (using modifiers such as "quartz," "feldspar," "glauconite," "mica," "kaolinite," "zeolitic," "lithic," "calcareous," "gypsiferous," or "sapropelic." In addition, the provenance of rock fragments (particularly in gravels, conglomerates, and breccias) can be described by modifiers such as "volcanic," "lithic," "gneissic," and "plutonic." The fabric of a sediment can be described as well using major modifiers such as "grain-supported," "matrix-supported," and "imbricated." Generally, fabric terms are useful only when describing gravels, conglomerates, and breccias.

The composition of volcanoclastic grains is described by the major and minor modifiers *lithic* (rock fragments), *vitric* (glass and pumice), and *crystal* (mineral crystals). Modifiers can also be used to describe the compositions of the lithic grains and crystals (e.g., *feldspathic* or *basaltic*).

Classes of Chemical Sediments and Rocks

Chemical sediments are composed of minerals that formed by inorganic processes such as precipitation from solution or colloidal suspension, deposition of insoluble precipitates, or recrystallization. Chemical sediments generally have a crystalline (i.e., nongranular) texture. There are five classes of chemical sediments: (1) *carbonaceous* sediments and rocks, (2) *evaporites*, (3) *silicates*, (4) *carbonates*, and (5) *metalliferous* sediments and rocks.

Carbonaceous sediments and rocks contain more than 50% organic matter (plant and algal remains) that has been altered from its original form by carbonization, bituminization, or putrefaction. Examples of carbonaceous sediments include peat, coal, and sapropel (jelly-like ooze or sludge of algal remains). The *evaporites* are classified according to their mineralogy using terms such as "halite," "gypsum," and "anhydrite." They may be modified by terms that describe their structure or fabric, such as "massive," "nodular," and "nodularmosaic." *Silicates* and *carbonates* are defined as crystalline sedimentary rocks that are nongranular and nonbiogenic in appearance. They are classified according to their mineralogy, using principal names such as "chert" (microcrystalline quartz), "calcite," and "dolomite." They should also be modified with terms that describe their crystalline

Millimeters	Microns	PRI (ϕ)	Wentworth size class	
4096		-20		
1024		-12	Boulder (-8 to -12 ϕ)	
256		-10		Gravel
64		-8	Cobble (-6 to -8 ϕ)	
16		-4	Pebble (-2 to -6 ϕ)	
4		-2		
3.36		-1.75		
2.83		-1.5	Granule	
2.38		-1.25		
2.00		-1.0		
1.68		-0.75		Very coarse sand
1.41		-0.5		
1.19		-0.25		
1.00		0.0		
0.84		0.25		Coarse sand
0.71		0.5		
0.59		0.75		
1/2	500	1.0		
0.42	420	1.25		
0.35	350	1.5	Medium sand	Sand
0.30	300	1.75		
1/4	250	2.0		
0.210	210	2.25		
0.177	177	2.5	Fine sand	
0.149	149	2.75		Very fine sand
1/8	125	3.0		
0.105	105	3.25		
0.088	88	3.5		
0.074	74	3.75		
1/16	63	4.0		Coarse silt
0.053	53	4.25		
0.044	44	4.5		
0.037	37	4.75		
1/32	31	5.0	Medium silt	
1/64	15.6	6.0	Fine silt	
1/128	7.8	7.0	Very fine silt	
1/256	3.9	8.0		
0.0020	2.0	9.0		
0.00098	0.96	10.0		
0.00049	0.49	11.0		
0.00024	0.24	12.0	Clay	
0.00012	0.12	13.0		
0.00006	0.06	14.0		

Figure 9. Udden-Wentworth grain-size classification of terrigenous sediments (from Wentworth, 1922).

(as opposed to granular) nature, such as "crystalline," "microcrystalline," "massive," and "amorphous." *Metalliferous* sediments and rocks are nongranular nonbiogenic sedimentary rocks that contain metal-bearing minerals such as pyrite, goethite, manganese oxyhydroxides, chamosite/berthierine, and glauconite. They are classified according to their mineralogy. This differs from Lisitzin et al. (1990), who defined metalliferous sediments as mixed sediment containing pelagic grains (often the major component) and material formed by precipitation from hydrothermal fluids.

Alteration of Carbonate Rocks

For the description of porosity in carbonate rocks, we use Choquette and Pray's (1970) classification (Fig. 10). The most common types of porosity encountered in the rocks drilled on Leg 144 are

1. *interparticle*: the space remaining between grains in ordinary sedimentary packing;
2. *intraparticle*: most commonly the space within components, such as the living chambers in a shell;
3. *fenestral*: a gap in the rock framework that is larger than the grain interstices;
4. *mollic*: formed by selective dissolution of individual particles;
5. *vuggy*: dissolution pores larger than individual grains.

The most important attributes of porosity are spelled out in text and, when appropriate, may be followed by Choquette and Pray's (1970) porosity notation. This notation, fully defined in Figure 10, generally includes more detail than the text descriptions.

Carbonate cements identified in visual and thin section descriptions are described using the terminology and notations of Folk (1965). As with porosity, the most important attributes of a cement are spelled out in text followed by a more complete description using the standard published code described in Tables 2 and 3.

BIOSTRATIGRAPHY

Time Scale—Chronological Framework

The Cenozoic chronostratigraphy used on Leg 144 follows that of Berggren, Kent, and Flynn (1985) and Berggren, Kent, and van Couvering (1985) for correlation of magnetostratigraphy, biostratigraphy, and the geochronological scale. The Cretaceous chronostratigraphy (Fig. 11) follows that of Harland et al. (1990). Throughout this volume, "m.y." denotes duration in millions of years whereas "Ma" denotes an absolute age in million of years.

Biostratigraphy

Preliminary age assignments were based on biostratigraphic analyses of calcareous nannofossils, planktonic and benthic foraminifers, diatoms, and dinoflagellates. All core-catcher samples and several additional samples within cores were analyzed.

Calcareous Nannofossils

The zonation of Okada and Bukry (1980) was used on Leg 144 for the Cenozoic calcareous nannofossils. This zonation, developed originally from sections in the equatorial Pacific (Bukry, 1973, 1975), is preferable to the land-based zonation of Martini (1971) because of the former's emphasis on oceanic nannofossil assemblages. Alternative zonal/subzonal indicators as well as secondary (intra-zonal) biohorizons have been used to improve stratigraphic resolution where feasible. Unless otherwise noted in the text, these additional biohorizons are based on the compilation of Perch-Nielsen (1985b). For the Pleistocene we adopted the modifications to the standard zonation proposed by Gartner (1977) and Rio et al. (1990) to improve the chronostratigraphic resolution of this interval.

In the Upper Cretaceous, the zonation of Sissingh (1977) was applied, with additional events proven to be useful at low latitudes (Perch-Nielsen, 1985a) (Fig. 11). The zonation of Thierstein (1971, 1973) was followed for the Lower Cretaceous, with modifications for the Albian as proposed by Roth (1978) (Fig. 11). We also adopted additional events calibrated with magnetostratigraphy and the planktonic foraminifer zonation (Perch-Nielsen, 1985a; Bralower, 1987; Channell and Erba, 1992; Coccioni et al., 1992).

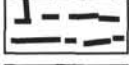
Basic porosity types			
Fabric selective		Not fabric selective	
	Interparticle	BP	
	Intraparticle	WP	
	Intercrystal	BC	
	Moldic	MO	
	Fenestral	FE	
	Shelter	SH	
	Growth-framework	GF	
			
			Fracture
			FR
			
			Channel*
			CH
			
			Vug*
			VUG
			
			Cavern*
			CV
			*Cavern applies to man sized or larger pores of channel or vug shapes.
Fabric selective or not			
	Breccia BR		Boring BO
			Burrow BU
			Shrinkage SK
Modifying terms			
Genetic modifiers		Size* modifiers	
Process	Direction or stage	Classes	
Solution = s	Enlarged = x	Megapore mg	mm ‡
Cementation = c	Reduced = r	Large lmg	256
Internal sediment = i	Filled = f	Small smg	32
		Mesopore ms	4
		Large lms	1/2
		Small sms	1/16
		Micropore mc	
Time of formation		Use size prefixes with basic porosity types: Mesovug = msVUG Small mesomold = smsMO Microinterparticle = mcBP	
Primary = P		*For regular-shaped pores smaller than cavern size.	
Predepositional = Pp		‡ Measures refer to average pore diameter of a single pore or the range in size of a pore assemblage. For tubular pores use average cross-section. For platy pores use width and note shape.	
Depositional = Pd			
Secondary = S			
Eogenetic = Se			
Mesogenetic = Sm			
Telogenetic = St			
Genetic modifiers are combined as follows: Process + Direction + Time		Abundance modifiers	
Examples: Solution-enlarged = sx Cement-reduced primary = crP Sediment-filled eogenetic = rfSe		Percent porosity (15%) or Ratio of porosity types (1:2) or Ratio and percent (1:2) (15%)	

Figure 10. Porosity types, modifying terms, and codes used to describe carbonate rock porosity on Leg 144 (from Choquette and Pray, 1970).

Table 2. Table of crystal size codes used for calcite cements in carbonate rocks (from Folk, 1965).

Size (mm)	Name	Symbol
4.0	Extremely coarsely crystalline (ECxn)	7
1.0	Very coarsely crystalline (VCxn)	6
0.25	Coarsely crystalline (Cxn)	5
0.062	Medium crystalline (Mxn)	4
0.016	Finely crystalline (Fxn)	3
0.004	Very finely crystalline (VFxn)	2
0.001	Aphanocrystalline (Axn)	1

Note: If the crystal size is transitional or widely varying, one can use such symbols as P.E24, D.F24, etc.

Table 3. Summary of codes used for calcite cements in carbonate rocks (from Folk, 1965).

I. Mode of formation	
P	= passive precipitation
P	= normal pore filling
P _s	= solution-fill
D	= displacive precipitation
N	= neomorphism
N	= as a general term, or where exact process unknown
N _i	= inversion from known aragonite
N _r	= recrystallization from known calcite
N _d	= degrading (also N _{id} and N _{rd})
N _s	= original fabric strained significantly
N _c	= coalescive (as opposed to porphyroid)
	(the above may be combined as N _{ids})
R	= replacement
II. Shape	
E	= equant, axial ratio <1½:1
B	= bladed, axial ratio 1½:1 to 6:1
F	= fibrous, axial ratio >6:1
III. Crystal size	
	Class 1, 2, 3, 4, 5, 6, or 7
IV. Foundation	
O	= overgrowth, in optical continuity with nucleus
O	= ordinary
O _m	= monocrystal
O _w	= widens outward from nucleus
C	= crust, physically oriented by nucleant surface
C	= ordinary
C _w	= widens outward from nucleus
S	= spherulitic with no obvious nucleus (fibrous or bladed calcite only)
	No symbol = randomly oriented, no obvious control by foundation

Planktonic Foraminifers

The Neogene tropical zonation of Blow (1969), as modified by Kennett and Srinivasan (1983), is used for Leg 144 sediments. The N7/N8 boundary is taken to be the first appearance of *Praeorbulina sicana*. The Oligocene/Miocene boundary, between Subzones N4a and N4b, is taken to be the first diversification of *Globigerinoides*, which occurs close to the first appearance of *Globoquadrina dehiscens*. The upper Eocene through Oligocene is subdivided according to the tropical zonation of Blow (1969). The Paleocene through middle Eocene is subdivided according to the scheme of Berggren, Kent, and Flynn (1985), as further explained by Berggren and Miller (1988). For the Mesozoic, the zonation of Caron (1985) is used. The *Globigerinelloides blowi*

and *G. duboisi* zones are placed (Fig. 11) according to Coccioni et al. (1992) and personal observations (I. Premoli Silva).

Larger Benthic Foraminifers

Figure 11 shows the major Cretaceous bioevents among larger benthic foraminifers plotted against planktonic zones and magnetostratigraphy, as adopted by Leg 144. These correlations between larger benthic foraminifer events and planktonic zones or magnetic chrons must be considered preliminary. The succession of events among the larger benthic foraminifers within the Lower Cretaceous through Turonian interval is based mainly on Arnaud et al. (1981) and a distribution chart prepared by the Working Group on Benthic Foraminifera of the IGCP Project No. 262, "Tethyan Cretaceous Correlation." A portion of this distribution chart will be published in the "Mesozoic-Cenozoic Chart of the European Basins," presented at the Dijon Meeting in May 1992. The complete chart will be published as part of the final report of the IGCP Project 262.

From the Turonian to the top of the Cretaceous, the correlation between larger benthic foraminifer events and planktonic zones, and then to magnetic chrons, is mainly based on van Gorsel (1978) and on the recovered material from the Marshall Islands (Lincoln et al., in press) and Nauru Basin (see also Premoli Silva and Brusa, 1981, for discussion).

Figure 12 shows the multiple zonation schemes for the Paleocene through Eocene based on *Assilina*, *Alveolina*, and several *Nummulites* lineages, and calibrated by calcareous nannofossils as proposed by Schaub (1981). These zonal schemes, established for the Tethys, seem to apply also to the faunas recovered in the western equatorial Pacific.

Diatoms and Siliceous Microfossil Groups

The combined low-latitude zonation for the Pacific Ocean of Burckle (1972) and Barron (1985) is used for the Neogene. Most of the Neogene diatom zones are correlated directly to the paleomagnetic record.

Palynomorphs

Numerous regional dinoflagellate biozonal schemes are available for the Cenozoic and Mesozoic (see summaries by Williams and Bujak, 1985, and in Powell, 1990), but most of these are based on neritic assemblages, and no standard zonal schemes exist.

Knowledge of oceanic assemblages in the North Atlantic realm has increased in recent years, especially for the Upper Cenozoic (e.g., de Vernal and Mudie, 1989a, 1989b; Head et al., 1989a, 1989b, 1989c; Manum et al., 1989; Mudie, 1989) and Paleogene (e.g., Manum et al., 1989; Head and Norris, 1989; Damassa et al., 1990), in which dinoflagellate zones are often constrained by nannofossils and in some cases by magnetostratigraphy. Few data exist for Pacific oceanic assemblages. Therefore, North Atlantic ranges are applied to Leg 144 material with caution.

For the Mesozoic, the general approach was to use global ranges compiled by Williams and Bujak (1985). A palynological zonation of Australia by Helby et al. (1987) was considered broadly applicable because of the more southerly latitude of the Leg 144 sites at that time, but this zonation is designed for neritic sediments and is of uncertain value for oceanic assemblages.

Methods and Procedures

Calcareous Nannofossils

The nannofossil assemblages were analyzed in smear slides prepared from raw sediment samples. Gravity settling was applied in a few cases to concentrate sparse nannofossil assemblages in critical intervals. Slides were observed with the light microscope,

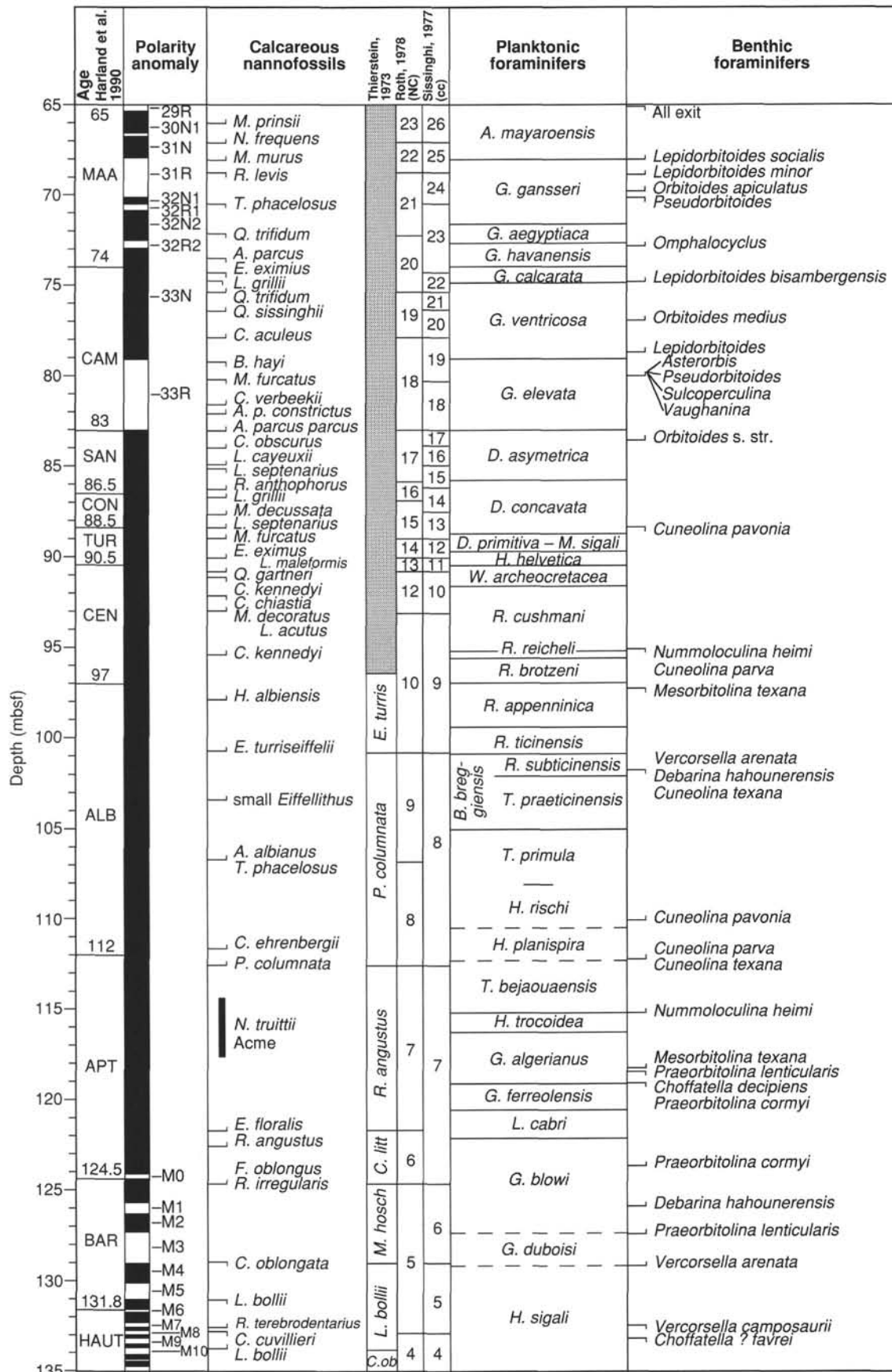


Figure 11. Barremian to Maastrichtian geochronology adopted during Leg 144.

Stage	Nummulites			Assilina	Alveolina	Calcareous nannofossils	Age
	<i>N. brongniarti</i> group	<i>N. perforatus</i> group	Others				
lower Oligocene			<i>fitcheli</i>				early Oligoc.
Priabonian			<i>fabianii</i>		(<i>Neoalveolina</i>)	<i>I. pseudoradians</i> <i>I. recurvus</i>	late
Biarritzian	<i>brongniarti</i>	<i>perforatus</i>	<i>ptukhiani</i>		<i>elongata</i>	<i>C. oamaruensis</i>	
Lutetian	upper	<i>herbi</i>	<i>aturicus</i>	<i>bullatus</i>	<i>gigantea</i>	?	<i>D. tani nodifer</i>
	middle 2	<i>sordensis</i>	<i>crassus</i>		<i>planospira</i>	<i>prorrecta</i>	
	middle 1	<i>gratus</i>	<i>beneharnensis</i>		<i>spira spira</i>	<i>munieri</i>	<i>C. alatus</i>
	lower 2 lower 1	<i>laevigatus</i>	<i>obesus</i> <i>gallensis</i>		<i>spira abrardi</i>	<i>stipes</i>	
Cuisian	upper	<i>manfredi</i>	<i>campesinus</i>	<i>formosus</i>	<i>maior</i>	<i>violae</i>	<i>D. sublodoensis</i>
	middle	<i>praelaevigatus</i>	<i>burd. cantabricus</i>	<i>nitidus</i>	<i>laxispira</i>	<i>dainellii</i>	<i>D. lodoensis</i>
	lower 2 lower 1	<i>planulatus</i>	<i>burdigalensis</i> <i>burdigalensis</i>	aff. <i>laxus</i>	<i>plana</i>	<i>oblonga</i>	<i>M. tribrachiatus</i>
Ilerdian	upper	<i>involutus</i>	<i>pernotus</i>	<i>laxus</i>	<i>adrianensis</i>	<i>trepmina</i>	<i>D. binodosus</i>
	middle 2	<i>exilis</i>		<i>globulus</i>	<i>leymeriei</i>	<i>corbarica</i>	
	middle 1	<i>robustiformis</i>	<i>carcasonensis</i>	aff. <i>arenensis</i>	<i>moussoulensis</i>	<i>M. contortus</i>	
	lower 2	<i>fraasi</i>	<i>solitarius</i>	<i>minervensis</i>	<i>arenensis</i>	<i>ellipsoidalis</i>	<i>D. multiradiatus</i>
	lower 1			<i>deserti</i>	<i>prisca</i>	<i>cucumiformis</i>	
Thanetian	upper				<i>yvettae</i>	<i>levis</i>	late
	lower					<i>primaeva</i>	
Danian						<i>E. macellus</i> <i>C. danicus</i> <i>C. tenuis</i> <i>M. inversus</i>	early

Figure 12. Paleocene through Eocene large benthic foraminifer correlation scheme (modified after Schaub, 1981) adopted during Leg 144.

at 1250× magnification. Estimates of the total nannofossil abundance were determined as follows:

- A (abundant): >10% of all particles;
- C (common): 1%–10% of all particles;
- F (few): 0.1%–1% of all particles;
- R (rare): <0.1% of all particles; and
- B (barren): no nannofossils.

Estimates of the preservation are coded as follows:

- G (good): little or no overgrowth/dissolution of most specimens;
- M (moderate): most specimens display moderate overgrowth/dissolution, and species identification is usually not impaired;
- P (poor): most specimens display significant amounts of overgrowth/dissolution, and species identification is sometimes impaired; and
- VP (very poor): all specimens display a significant amount of overgrowth/dissolution, and species identification is usually impaired.

Estimates of the relative abundance of calcareous nannofossil species in pelagic/hemipelagic assemblages were determined as follows:

- D (dominant): >30 specimens/field of view at 1250×;
- A (abundant): 10–30 specimens/field of view at 1250×;
- C (common): 1–10 specimens/field of view at 1250×;
- F (few): 1 specimen/2–10 fields of view at 1250×;
- R (rare): 1 specimen/11–100 fields of view at 1250×; and
- VR (very rare): 1 specimen/>100 fields of view at 1250×.

Foraminifers

Samples from pelagic sediments were prepared by washing over 150- and 45-µm mesh sieves and drying on a hot plate. Consolidated sediments were soaked in hydrogen peroxide or Calgon and then boiled or treated ultrasonically before being washed and dried.

The abundance of a particular species within a sample is based on a visual estimation of the >150-µm size fraction. The following letters indicate abundance estimates:

- A (abundant): >30% of the fauna;
- C (common): 15%–30%;
- F (few): 3%–15%; and
- B (barren).

The preservation state of the planktonic foraminifer assemblage is estimated as follows:

G (good): little or no evidence of overgrowth, dissolution, or abrasion;

M (moderate): calcite overgrowth, dissolution, or abrasion are common but minor; and

P (poor): substantial overgrowth, dissolution, or fragmentation.

Samples from limestones were viewed in thin section or in acetate peels. Acetate peels were prepared by first polishing the surfaces, then etching them with 2% HCl. After immersion in the HCl solution, the surfaces were rinsed thoroughly under running water. Once dried, the surfaces were flooded with acetone and immediately covered with acetate film, then pressed evenly to assure smooth adhesion of the film to the surface. After a few hours of drying, the acetate films were peeled off. Oriented thin sections were also prepared for isolated specimens of larger foraminifers. The relative abundance of benthic foraminifers in thin section is estimated as follows:

A (abundant): >10 for larger foraminifers, and >20 for small foraminifers;

C (common): 6–10 for larger foraminifers, and 10–20 for small foraminifers;

F (few): 3–5 for larger foraminifers, and 3–10 for small foraminifers;

R (rare) = 2 specimens (for both larger and small foraminifers); and

S (single) = single specimens (for both larger and small foraminifers).

Diatoms, Siliceous Microfossil Groups, and Authigenic Minerals

Slides for quantitative analysis were prepared by distributing a defined aliquot of the homogenized suspension of the HCl-insoluble residue of a dried and weighed sediment sample onto a 17.5 × 17.5 mm coverslip. Hyrax (refractive index n.d. = 2.71) was used as the mounting medium.

The abundance of siliceous microfossil groups and authigenic minerals was calculated as numbers/gram sediment based on counting five traverses across the slide. The relative abundances of diatom species were recorded semiquantitatively using the following categories:

S (single): <1%;

R (rare): 1%–5%;

F (few): 5%–10%;

C (common): 10%–30%;

A (abundant): 30%–50%; and

D (dominant): >50%.

Estimates of diatom preservation were based on the degree of etching and fragmentation of the diatom valves in connection with the relative abundance of more dissolution-resistant species.

Palynomorphs

Samples were first cleaned of adherent cutting or drilling slurry, and one or two *Lycopodium clavatum* tablets (Batch no. 710961, around 1400 spores per tablet; available from the Department of Quaternary Geology, University of Lund, Sweden) were added to each sample to provide qualitative control over processing losses and damage. Each sample was then treated with 10% HCl and washed in distilled water. HCl digestion was found to be adequate by itself to concentrate organic residues from carbonate samples, but other lithologies including clays were subsequently treated with hot or cold 48% HF followed by further HCl. The organic residue was then sieved through 10- or 20- μ m Nitex mesh screens to concentrate any palynomorphs that might be present; these were mounted on a microscope slide using glycerine jelly.

An unsieved kerogen slide was also made to assist in evaluation of the palynofacies. Brief (up to 1 min) ultrasonification was occasionally used to concentrate palynomorphs before sieving. The relative abundance of palynomorphs was estimated as follows:

A (abundant): >1 specimen/field of view at 100 \times ;

C (common): >1 specimen/2–15 fields of view at 100 \times ;

R (rare): >1 specimen/16–50 fields of view at 100 \times ; and

S (single): 1 specimen/22 × 40 cm slide.

Estimates of preservation are indicated as follows:

G (good): no signs of corrosion;

M (moderate): fine details not preserved;

P (poor): extensive corrosion.

PALEOMAGNETISM

Magnetic measurements during Leg 144 varied with lithology, coring method, and amount of recovery. Continuous remanence measurements of some APC cores were made with the cryogenic pass-through magnetometer. The natural remanent magnetization (NRM) and magnetization after demagnetization at 15 mT were routinely recorded at a 5-cm spacing. Drilling disturbance was severe in many cores from the pelagic cap, and measurements were discontinued in these portions of the section. For material obtained with the rotary core system, recovery was often too low to allow routine measurement of remanence with the pass-through magnetometer. The primary shipboard paleomagnetic scanning technique was the measurement of standard minicores (2.54-cm diameter) or 1-in. cubes. Longer continuous core pieces from the archive halves of split cores were also occasionally measured in the cryogenic pass-through magnetometer, both from the limestone and basalt intervals at each site. Magnetic susceptibility was measured at 5- or 10-cm intervals for APC cores but was restricted to intervals of good recovery in the limestone and basalt sequences.

Instruments

Magnetic remanence on Leg 144 was measured with the shipboard 2-G Enterprises (Model 760R), three-axis, pass-through cryogenic magnetometer. The SQUID sensors measure magnetization over an interval approximately 20 cm long, with each axis having a slightly different response curve. The data were not deconvolved. Rather, declination and inclination were calculated from the three-axis measurements by dividing the magnetic moment by the effective volume within the sensing region. The magnetometer has an on-line alternating field demagnetizer (Model 2G600) capable of alternating fields up to 20 mT, although ODP policy limits demagnetization of the archive sections to 15 mT. Alternating-field (AF) demagnetization was limited to those archive sections in which the NRM measurements indicated that the remanence was stable and the intensity was above the lower practical limit of operation of the shipboard cryogenic pass-through magnetometer (about 0.01 mAm⁻¹ for a half core).

The cryogenic pass-through magnetometer was operated in two modes. Standard pass-through measurements were made on archive core halves, and a discrete sample measurement program allowed measurement of up to seven samples during a single run. We measured a maximum of four discrete samples at a time (in positions 1, 3, 5, and 7) to avoid any possible effect of the slight overlap in response functions at a spacing of approximately 20 cm. Most discrete samples were demagnetized (to a maximum of 90 mT) using the Schonstedt Model GSD-1 AC demagnetizer. A spurious anhysteretic remanent magnetization (ARM) may be imparted at the higher levels of demagnetization. Successive demagnetization steps, therefore, were made along opposing axial directions to detect the acquisition of a spurious ARM. Intermit-

tent problems with the Schonstedt demagnetizer necessitated using the 2G demagnetizer for some discrete samples. Although it was possible to make discrete sample measurements using a Molspin spinner magnetometer, we found that samples with intensities greater than 15 Am^{-1} (for $10\text{--}12 \text{ cm}^3$ volume) could be measured with the cryogenic magnetometer, and thus the Molspin experienced limited use.

Cross calibration of the three axes of the cryogenic pass-through magnetometer was achieved by measuring several standards with essentially uniaxial magnetization. Ideally, the same magnetic moment should be recovered regardless of the sensor used or the sample orientation. We found, however, that the z -axis intensity was underestimated by approximately 10%–12% relative to the horizontal axes; therefore, inclination estimates were systematically too shallow, by about 4° at 45° inclination. This effect is smaller at both higher and lower inclinations. Inclination data reported in table form are uncorrected, although mean inclinations and tentative paleolatitude estimates for sites have been corrected. Revised calibration constants will be incorporated into the cryogenic programs after additional testing.

Magnetic susceptibility of whole-core sections was measured as part of the physical properties "MST" package with a Bartington Instruments magnetic susceptibility meter (Model M.S.1, using a M.S.1/CX 80-mm whole-core sensor loop). Susceptibility measurements on selected discrete samples were made using the corresponding Bartington M.S.1.B meter.

Data Analysis

The magnetization of many of the sediments was very weak, frequently $<0.1 \text{ mAm}^{-1}$. Measurement of discrete specimens from many intervals was reserved, therefore, for shore-based studies, where more sensitive magnetometers would be available. Demagnetization of more strongly magnetized sediments and basalts allowed the directions of the characteristic remanent magnetization (ChRM) of these materials to be isolated on board. Analysis of inclination-only data should account for the underestimation of the mean inclination derived from azimuthally unoriented cores (e.g., McFadden and Reid, 1982). Because software for this analysis was not available, the arithmetic mean of inclination values (or sequential "virtual inclination" groups where practical) was used to estimate the paleolatitude. We consider these paleolatitude estimates to be preliminary and a guide to further work.

Time Scales

For the Cenozoic, correlations between biostratigraphic zonations and magnetic reversals and absolute ages are based on the time scale of Berggren, Kent, Flynn, and van Couvering (1985). The Mesozoic chronostratigraphy follows that of Harland et al. (1990). Correlations between the various Cretaceous biostratigraphic zonations and the magnetic reversal sequence are illustrated in the "Biostratigraphy" section (this chapter).

INORGANIC GEOCHEMISTRY

During Leg 144, three additions were made to the routine shipboard inorganic geochemistry program: (1) interstitial waters were analyzed for their fluoride concentration; (2) routine shipboard methods for processing interstitial waters were modified to reduce seawater contamination of interstitial waters in highly porous foraminifer sands; and (3) limestone samples were taken from selected cores and analyzed for calcium, magnesium, fluoride, silica, strontium, phosphate, iron, and manganese.

Interstitial Water Chemistry

The shipboard inorganic geochemistry program focused on the retrieval of interstitial waters by means of hydraulic-press-actuated extrusion of samples obtained from 5- to 10-cm-long, whole-

round or half-round core sections. Immediately after retrieval of the core on deck, it was cut into sections and the whole-rounded core samples for inorganic geochemistry were taken before the sections were sealed using acetone with plastic end caps. Additional precautions were followed to minimize the effects of core contamination by drill water or drilling mud. The exteriors, as well as the cracks and fissures, of these core samples were carefully scraped with spatulas to remove potentially contaminated surfaces before they were placed into stainless steel presses and placed into a hydraulic squeezer, as described by Manheim and Sayles (1974). Under pressure, the interstitial waters flowed through $0.45\text{-}\mu\text{m}$ Gelman acrodisc disposable filters into plastic syringes, where they subsequently subdivided for shipboard work as well as for future work in shore-based laboratories. Special attention was given to taking closely spaced samples in the upper 100 m (one whole-round core sample per core), followed by one sample every third core.

Excessive seawater contamination of pore fluids in highly porous foraminifer sands at Sites 871 and 872 prompted the application of a sequential squeezing technique at Site 873 when similar sediments were encountered. This technique involved discarding the first 30 mL of interstitial water squeezed out of the sediment as a result of the application of a pressure of 2.5 metric tons. By slowly increasing pressure to a maximum of 18 tons in the "second squeeze," these sediments still yielded 40 to 50 mL of pore water (sufficient for shipboard and shore-based analyses). Results from Site 873 were sufficiently encouraging ("Site 873" chapter, this volume) for us to recommend that the sequential squeezing technique be employed on future legs where these sediments are encountered.

Interstitial water samples were routinely analyzed for salinity, pH, alkalinity, chlorinity, calcium, magnesium, sulfate, fluoride, silica, ammonium, sodium, potassium, strontium, rubidium, and lithium.

The routine measurements of the interstitial waters were performed as follows: salinities with a hand-held Goldberg optical refractometer; pH and alkalinity by Gran titration using a Brinkmann pH electrode and a Metrohm autotitrator; Cl^- , Ca^{+2} , and Mg^{+2} concentrations by titration; SO_4^{2-} with a DIONEX 2120i chromatograph; and F, Si, and NH_4 with colorimetric techniques using a Milton Roy Spectronic 1001 spectrophotometer.

The standard seawater of the International Association of Physical Sciences Organizations (IAPSO) was used to calibrate most of these techniques. Chemical data are reported in molar units.

Shipboard analyses performed are listed in Table 4. All these techniques were performed as described by Gieskes et al. (1991).

Lithologic Analysis

Rock samples were taken from samples of the split core using a hand-held drill and a 1.1-mm diameter bit. Approximately 20 mg of rock powder were weighed accurately, dissolved in 2 mL of 10% hydrochloric acid, and then diluted to 4 mL by adding deionized water. Concentrations of calcium, magnesium, strontium, manganese, and iron were determined using flame spectrophotometric techniques. Fluoride, silica, and phosphate concentrations were determined colorimetrically using a Milton Roy Spectronic 1001 spectrophotometer. All data were expressed as molar ratios to calcium: $(\text{Mg}/\text{Ca} \cdot 10^2)$, $(\text{Sr}/\text{Ca} \cdot 10^3)$, $(\text{F}/\text{Ca} \cdot 10^3)$, $(\text{PO}_4/\text{Ca} \cdot 10^3)$, $(\text{SiO}_2/\text{Ca} \cdot 10^3)$, $(\text{Fe}/\text{Ca} \cdot 10^3)$, and $(\text{Mn}/\text{Ca} \cdot 10^4)$.

Atomic Absorption/Emission Analysis

The AA procedures used on ODP cruises have been described in detail by Gieskes et al. (1991) and in the Leg 133 "Explanatory Notes" chapter (Davies, McKenzie, Palmer-Julson, et al., 1991). We used flame spectrophotometric techniques with a Varian

SpectrAA-20 atomic absorption unit to quantify concentrations of Na, K, Li, Sr, and Rb in interstitial water samples and Ca, Mg, Sr, Mn, and Fe in rock samples. Standards for analyzing potassium and sodium were prepared by diluting IAPSO (399.43 ppm K) with distilled (nanopure) water. The 1/200 diluted aliquots, which remain from SO_4^{2-} analysis, were used to prepare the final dilution (1/10) and were analyzed by flame emission using an air-acetylene flame (Varian AA at 766.5-nm wavelength) with 3.5% CsCl solution as an ionization suppressant.

Lithium was determined on 1/30 diluted aliquots by emission using an air-acetylene flame. Standards were prepared from a LiCl_2 (50 mM) solution.

Strontium was measured in the absorption mode at 460.7 nm using an air-acetylene flame. Standards were prepared using stock 1000 ppm Sr solution. Standards of 1, 2, 5, 10, and 15 ppm were prepared. Strontium was analyzed on a 1:20 solution of the samples, whereby lanthanum trichloride (50,000 ppm) was used as a background buffer in the sample solution. This method was found to provide reproducible results for interstitial water samples and rock samples.

Rubidium was determined directly on undiluted interstitial water samples by emission using an air-acetylene flame. Standards were prepared from a 100 ppm Rb reference solution. Standards for all flame spectrophotometric techniques were matched in matrix composition to the samples.

Calcium was measured in the absorbance mode on 1/400 diluted aliquots of the rock powder solution at 422.7 nm using an air-acetylene flame. Magnesium was measured in the absorbance mode on 1/300 diluted aliquots of the rock powder solution at 285.2 nm using an air-acetylene flame. Values for Mn and Fe were determined directly on undiluted rock powder solutions at 403.1 and 372 nm, respectively, in the emission mode using a nitrous oxide-acetylene flame.

ORGANIC GEOCHEMISTRY

Shipboard organic geochemistry for Leg 144 included the following analyses: (1) determination of total carbonate carbon in whole rock; (2) elemental analyses of carbon, nitrogen, hydrogen, and sulfur in whole-rock and acid residues from carbonates; (3) determination of free hydrocarbons, petroleum potential, and thermal maturity of organic matter; (4) analyses of hydrocarbon gases; and (5) pyrolysis gas chromatography on organic matter. Detailed procedures are described by Emeis and Kvenvolden (1986).

Table 4. Analytical methods used during Leg 144.

Analysis	Technique	Reference
Salinity	Goldberg refractometer	
Alkalinity	Gran titration	Dyrssen (1965)
pH	TRIS-BIS buffers	Bates and Calais (1981); Bates and Culbertson (1977)
Calcium	EGTA titration	Tsunogai et al. (1968)
*Calcium	Absorption spectrometry	
Magnesium	EDTA titration	Grasshoff et al. (1983)
*Magnesium	Absorption spectrometry	
Strontium	Absorption spectrometry	
Rubidium	Emission spectrometry	
Lithium	Emission spectrometry	
Sodium	Emission spectrometry	
Potassium	Emission spectrometry	
*Manganese	Emission spectrometry	
*Iron	Emission spectrometry	
Chlorinity	Mohr titration	
Ammonia	Colorimetry	Solorzano (1969); Gieskes (1973)
Silica	Colorimetry	Gieskes (1973)
Fluoride	Colorimetry	Carpenter (1969)
*Phosphate	Colorimetry	Presley, 1971

Note: Analytical methods from Gieskes et al. (1991).

*Used for rock samples only.

Inorganic Carbon

Determination of total organic carbon in sediments is normally performed by subtraction of inorganic carbon from total carbon. In sedimentary rocks, virtually all inorganic carbon is confined to carbonate minerals. Therefore, we decided to include the carbonate carbon analysis method as part of the organic geochemistry program. In the following, "inorganic carbon" is used synonymously with carbonate carbon.

Inorganic carbon was determined using a Coulometrics 5011 carbon dioxide coulometer equipped with a System 140 carbonate carbon analyzer. Freeze-dried and weighed samples of between 10 and 20 mg were reacted in 2N HCl solution at 60°C. Evolved carbon dioxide was titrated in a monoethanolamide solution with a coulometric indicator over a period of 5 to 20 min depending on carbonate reactivity. Calibration was performed using pure calcium carbonate as a standard. The percentage of carbonate was calculated from the inorganic carbon (IC) content, assuming that all carbonate was in the form of calcite:

$$\text{CaCO}_3 = \text{IC} \cdot 8.332.$$

No corrections were made for siderite or dolomite. Standard deviation for ten consecutive standard runs was better than 1.5%.

Total nitrogen, carbon, hydrogen, and sulfur contents of whole-rock samples were determined using a Carlo Erba NCS-analyzer, model NA 1500. Freeze-dried and crushed samples of between 2 and 10 mg were mixed with vanadium pentoxide and combusted in an oxygen atmosphere at 1000°C. With this technique, organic and inorganic carbon were converted to carbon dioxide, sulfur to sulfur dioxide, and nitrogen to nitrogen dioxide, which was further reduced to nitrogen gas using copper as a reducing agent. The hydrogen was trapped as water. The gases were separated by gas chromatography and measured with a thermal conductivity detector. Total organic carbon (TOC) was calculated from the difference between total carbon (TC) determined by elemental analyses and inorganic carbon (IC) determined by coulometry according to the formula:

$$\text{TOC}\% = \text{TC}\% - \text{IC}\%.$$

The precision of TOC determinations is defined by the combined precision of the TC and IC methods and is generally not better than 2%.

Organic Matter Characterization and Maturation

On Leg 144, two pyrolysis instruments were available for the rapid characterization of organic matter type and maturity: (1) a Delsig-Nermag Rock-Eval II (RE) (Espitalié et al., 1985a, 1985b, 1986) with total organic carbon facility, and (2) a Geofina Hydrocarbon Meter (GHM). Both instruments use temperature-programmed, whole-rock pyrolysis techniques to determine the amount of volatile hydrocarbons (S_1 mg hydrocarbons/g of sediment) and pyrolyzable hydrocarbons (S_2 mg hydrocarbons/g of sediment). The S_1 parameter is a measure of oil in the sediment, whereas the S_2 parameter indicates the oil potential of the rock. Both instruments also determine the temperature (T_{max} °C) of the maximal hydrocarbon formation (S_2 peak), which is a measure of thermal maturity of the sediment. In the Rock-Eval instrument, carbon dioxide produced from organic matter is trapped from 300° to 390°C and analyzed to give S_3 , which is reported as milligrams of carbon dioxide per gram of sediment. This parameter is generally used for the characterization of organic matter, but it may yield unreliable results in carbonate-rich rocks. Finally, the remaining organic matter in the sample is oxidized at a temperature of 600°C to yield additional data for the calculation of TOC.

Sample sizes used for the Rock-Eval are between 100 and 200 mg. The instrument was only available during the latter part of Leg 144 because of repairs.

The hydrogen index (HI) is the TOC-normalized amount of pyrolyzable organic matter or "hydrocarbons" as determined from the Rock-Eval S_2 peak and TOC value ($HI = S_2/TOC$ mg/g sample). This parameter is used to characterize and evaluate the hydrocarbon potential of the rock. The production index (PI) is defined as the ratio $S_1/(S_1 + S_2)$.

The Geofina Hydrocarbon Meter (GHM) pyrolysis-gas chromatographic instrument is based on a modified Varian 3400 gas chromatograph with three flame ionization detectors (FID), two capillary columns (25 m, GC2 fused silica), a sample injector for solid or liquid samples, and a temperature programmable oven. The instrument is comparable to the Rock-Eval for the determination of volatile hydrocarbons (S_1), pyrolyzable hydrocarbons (S_2), and T_{max} . Moreover, the standard use of the instrument includes gas chromatography of the hydrocarbons (S_1 and S_2) evolved during the pyrolysis procedure. This feature makes it possible to characterize the organic matter by pyrolysis-gas chromatography (PY-GC) techniques. The required sample size for the GHM instrument is 1–2 mg of organic matter.

Hydrocarbon Gases

For safety reasons, concentrations of the light hydrocarbon gases C_1 to C_3 (methane, ethane, and propane) were monitored in each core or whenever gas pockets were encountered. Gases were extracted using the head-space technique for bulk sediments, described by Kvenvolden and McDonald (1986), or by using the vacutainer for sampling gas pockets directly through the core liner. Head-space analyses were performed on 5 cm³ sediment samples heated in sealed vials at 70°C for 30 min before gas analysis. Immediately after retrieval and cutting of the core, a No. 6 cork borer with a calibrated plunger was used to obtain a measurable volume of sediment from the end of a core. All gas samples were analyzed on a Carle AGC series 100/Model 211 gas chromatograph. This instrument has a detection limit for methane of 0.1 ppm. The background concentration of methane was monitored regularly in the laboratory and on the core deck. Average values are between 2 and 3 ppm.

IGNEOUS PETROLOGY

Visual Core Descriptions

Visual core description (VCD) forms for "igneous and metamorphic rocks" were used in the documentation of the igneous rock cores (see core description forms and photographs at the back of this volume). The left column is a graphic representation of pieces comprising the archive half of the core. A horizontal line across the entire width of the column denotes a plastic spacer. Vertically oriented pieces are indicated on the form by an upward-pointing arrow to the right of the piece. Shipboard samples and studies are indicated in the column headed "Shipboard studies," using the following notation: XRD = X-ray diffraction analysis, XRF = X-ray fluorescence analysis, TSB = petrographic thin section, PP = physical properties analysis, and PMAG = paleomagnetic analysis.

To ensure consistent and complete descriptions, the visual core descriptions were entered into the computerized data base HARVI, which is divided into separate data sets for fine- and coarse-grained rocks. No coarse-grained rocks were recovered during Leg 144. Fine-grained rocks are either aphyric or phyrlic with a microcrystalline, aphanitic, or glassy matrix, whereas coarse-grained rocks are holocrystalline with groundmass minerals that are visible with the aid of a $\times 10$ hand lens. Each record is checked by the data-base program for consistency and complete-

ness and is subsequently printed in a format that can be pasted directly onto the barrel sheet for subsequent curatorial handling.

Each core was subdivided into lithologic units whose boundaries are defined by chilled, rubbly, or vesicular flow margins or by the presence of intervening soil or sedimentary horizons. Where flow boundaries were not recovered, lithologic units were defined on the basis of changes in phenocryst content and/or texture or because separated by intervals of broken and/or extensively altered material. In some cases, significant intervals of such material were also assigned unit numbers. For each lithologic unit and section, the following information was recorded in the data base:

1. Leg, site, hole, core number, core type, and section number.
2. Unit number (consecutive downhole), position in the section, number of pieces of the same lithologic type, the rock name, and the identification of the describer.
3. Mineral phases visible with a hand lens and their distribution within the unit, together with the following information for each phase: (a) estimated abundance (volume %); (b) size range in millimeters, (c) shape, (d) degree of alteration, and (e) further comments.
4. Groundmass texture: glassy, aphanitic or microcrystalline.
5. Secondary minerals and alteration products.
6. Vesicles and their infillings.
7. Massive thin or sheet flows, pillow lavas, sills, dikes, hyaloclastites, and brecciated layered or banded.
8. Characteristics of veins and fractures.
9. Other comments, including notes on the continuity of the unit within the core and on the interrelationship of units.

Basalts were named in order of phenocryst type (e.g., a plagioclase olivine phyrlic basalt contains mostly plagioclase, with subordinate olivine).

Volcaniclastic units were termed "breccia" if clast size was generally < 2 cm and "coarse breccia" if clast sizes were > 5 cm.

Igneous visual core descriptions are given in Section 3 at the back of this volume, and descriptions of each rock unit are available from the computerized data base at the ODP repositories.

Thin Section Descriptions

Thin sections of igneous rocks were examined to complement and refine the hand-specimen observations. The percentages and textural descriptions of individual phases are reported in the computerized data base HRTIN. The same terminology was used for both thin section and megascopic descriptions. Thin section descriptions are included in Section 3 at the back of this volume and are also available from the ODP computerized data base.

X-ray Fluorescence Analysis

Vein and vesicle fillings and other visibly altered material were physically removed from samples before they were crushed in a Spex 8510 shatterbox using a tungsten carbide barrel. At least 20 cm³ of material was ground to ensure a representative sample. The tungsten carbide barrel introduces considerable W contamination and minor Ta, Co, and Nb contamination, rendering the powder unsuitable for instrumental neutron activation analysis (INAA).

A fully automated wavelength-dispersive ARL8420 XRF (3 kW) system equipped with a Rh target X-ray tube was used to determine the major oxide and trace element abundances of whole-rock samples. Analyses of the major oxides were conducted on lithium borate glass disks doped with lanthanum as a "heavy absorber" (Norrish and Hutton, 1969). The disks were prepared from 500 mg of rock powder, ignited for 3–4 hr at about

1025°C, and mixed with 6.0 g of preweighed (on shore) dry flux consisting of 80% lithium tetraborate and 20% La₂O₃. This mixture was then melted in air at 1150°C in a Pt-Au crucible for about 10 min and poured into a Pt-Au mold using a Claisse Fluxer. The 12:1 flux-to-sample ratio and the use of the lanthanum absorber made matrix effects insignificant over the normal range of igneous rock compositions. Hence, the relationship between X-ray intensity and concentration becomes linear and can be described by:

$$C_i = (I_i \cdot m_i) - b_i,$$

where

C_i = concentration of element i (wt%);

I_i = net peak X-ray intensity of element i ;

m_i = slope of calibration curve for element i (wt%/cps); and

b_i = apparent background concentration for element i (wt%).

Slope, m_i , was calculated from a calibration curve derived from the measurement of well-analyzed reference rocks (BEN, BR, DRN [from Geostandards, France]; BHVO-1 and AGV-1 [from the U.S. Geological Survey]; JGB-1 and JP-1 [from the Geological Survey of Japan]; AII-92-29-1 [from Woods Hole Oceanographic Institution/Massachusetts Institute of Technology]; and K1919 [from Lamont-Doherty Geological Observatory]). The analyses of these standards, treated as unknowns against the calibration curves, are given in Table 5. Background, b_i , was determined by regression analysis from the calibration curves.

Systematic errors resulting from short- or long-term fluctuations in X-ray tube intensity and instrument temperature were corrected by normalizing the measured intensities of the samples to those of an internal standard that was run together with a set of six unknown samples. Two glass disks were prepared for each sample. Accurate weighing was difficult on board the moving *JOIDES Resolution*; measurements were performed with particular care, therefore, as weighing errors could be a major source of imprecision in the final analysis. Five weight measurements, with weights within 0.5 mg ($\pm 0.1\%$) considered acceptable, were taken for each sample and the average was used. Loss on ignition (LOI) was determined by drying the sample at 110°C for 8 hr, and then by weighing before and after ignition at 1025°C in air.

Trace element determinations were made on pressed-powder pellets prepared by pressing (with 8 MPa of pressure) a mixture of 5.0 g of dry rock powder (dried at 110°C for >2 hr) and 30 drops of polyvinyl alcohol binder into an aluminum cap. A modified Compton scattering technique, based on the intensity of the Rh Compton peak, was used for matrix absorption corrections (Reynolds, 1967).

Replicate analyses of rock standards show that the major element data are precise within 0.5% to 2.5%; they are considered accurate to ~1% for Si, Ti, Fe, Ca, and K, and between 3% and 5% for Al, Mn, Na, and P. The trace element data are considered accurate to within 2% and 3% or 1 ppm (whichever is greater) for Rb, Sr, Y, and Zr, and between 5% and 10% or 1 ppm for most of the others. The accuracy for Ba and Ce is considerably less, and they are primarily for purposes of internal comparison. Precision is within 3% for Ni, Cr, and V at concentrations >100 ppm, but from 10% to 25% for concentrations <100 ppm. Analytical conditions for the XRF analyses are given in Table 6.

PHYSICAL PROPERTIES

Shipboard measurements of physical properties provide the basis for characterizing lithologic units, correlating between various boreholes, and making comparisons with downhole logging

Table 5. Analyses of standards derived from the calibrations used for whole-rock analyses.

Sample run	BHVO published	BHVO ABJ	BHVO ABO	BHVO ABR	Mean (of 15)	1°
Major elements (wt%):						
SiO ₂	49.62	49.73	49.63	49.56	49.63	0.083
TiO ₂	2.68	2.74	2.73	2.74	2.74	0.009
Al ₂ O ₃	13.67	13.52	13.48	13.42	13.48	0.034
Fe ₂ O ₃	12.23	12.27	12.23	12.30	12.25	0.042
MnO	0.17	0.17	0.17	0.17	0.17	0.003
MgO	7.21	7.16	7.07	7.24	7.11	0.099
CaO	11.32	11.38	11.34	11.39	11.39	0.035
Na ₂ O	2.17	2.32	2.31	2.31	2.27	0.099
K ₂ O	0.53	0.51	0.49	0.49	0.49	0.015
P ₂ O ₅	0.27	0.23	0.20	0.19	0.20	0.017
Total	99.87	100.03	99.65	99.81	99.73	0.233
Sample run	BHVO AAP	BHVO AAQ	BHVO AAS	Mean (of 8)	1°	
Trace elements (ppm):						
Nb	19.7	20.2	20.1	20.3	0.4	
Zr	182.1	183.0	183.3	182.8	0.7	
Y	27.3	27.3	26.8	27.2	0.3	
Sr	403.0	407.7	403.7	405.5	2.7	
Rb	9.2	8.7	8.6	9.1	0.3	
Zn	108.6	108.7	109.0	109.0	0.6	
Cu	139.8	141.4	141.8	141.3	0.9	
Ni	124.9	125.2	126.1	125.0	1.0	
Cr	288.7	285.1	283.4	289.2	0.6	
V	323.2	314.4	313.8	319.1	5.1	
Ce	36.7	38.1	35.3	37.9	1.7	
Ba	120.6	122.7	113.9	119.3	5.8	

parameters. In addition, they provide an important link between the drilling results and geophysical site survey data.

Whole-round cores were allowed to equilibrate to room temperature for 2–4 hr before making any measurements of physical properties. Several types of nondestructive measurements were made on the whole-round core sections using the multisensor track (MST). Individual core sections were placed horizontally on the MST and then moved through three sets of sensors that measure wet-bulk density and porosity, compressional wave velocity, and magnetic susceptibility, respectively. These are (1) the gamma-ray attenuation porosity evaluator (GRAPE), (2) the P -wave logger (PWL), and (3) a magnetic susceptibility loop. Shipboard determinations of thermal conductivity were also made at discrete intervals in whole-round sections of unlithified sediment cores using the needle-probe method of von Herzen and Maxwell (1959).

Whole-round core sections were split lengthwise and then sampled with sufficient density to characterize the range of lithologic units recovered from each hole. Where necessary, because of closely spaced changes in lithology and/or physical properties, additional measurements were obtained. Discrete measurements of index properties (wet- and dry-bulk density, grain density, porosity, and water content), compressional wave velocities, and shear strength values were made at specific intervals along split core sections. For all discrete measurements of physical properties, an effort was made to analyze only "visually" undisturbed sediment and rock. The techniques that were used in the determination of index properties and compressional wave velocity are described in detail by Boyce (1976). Three different methods were used to measure sonic velocity, largely depending on the coherence and competence of the material, which varied from unlithified, to semi-indurated to well-lithified.

Multisensor Track

Gamma-ray Attenuation Porosity Evaluator (GRAPE)

The GRAPE technique measures bulk density and porosity in whole APC and XCB cores where the core liner is both unde-

Table 6. Analytical conditions for X-ray fluorescence, Leg 144.

Element	Line	Crystal	Detector	Collimator	Peak angle (degrees)	Background offset (degrees)	Total count time (ss)	
							Peak	Background
Major elements (wt%):								
SiO ₂	Kα	PET(002)	FPC	Coarse	109.04	0	40	0
TiO ₂	Kα	LiF(200)	FPC	Fine	86.17	0	40	0
Al ₂ O ₃	Kα	PET(002)	FPC	Coarse	144.47	0	100	0
Fe ₂ O ₃ *	Kα	LiF(200)	FPC	Fine	57.56	0	40	0
MnO	Kα	LiF(200)	KrSC	Fine	63.00	0	40	0
MgO	Kα	TLAP	FPC	Coarse	44.77	±0.80	200	400
CaO	Kα	LiF(200)	FPC	Coarse	113.14	0	40	0
Na ₂ O	Kα	TLAP	FPC	Coarse	54.61	1.20	200	200
K ₂ O	Kα	LiF(200)	FPC	Coarse	136.64	0	100	0
P ₂ O ₅	Kα	Ge(111)	FPC	Coarse	140.98	0	100	0
Trace elements (ppm):								
Rh	K-C	LiF(200)	Scint	Fine	18.63	0	60	0
Nb	Kα	LiF(200)	Scint	Fine	21.43	±0.35	200	200
Zr	Kα	LiF(200)	Scint	Fine	22.57	±0.35	100	100
Y	Kα	LiF(200)	Scint	Fine	23.82	±0.40	100	100
Sr	Kα	LiF(200)	Scint	Fine	25.17	±0.41	100	100
Rb	Kα	LiF(200)	Scint	Fine	26.63	±0.60	100	100
Zn	Kα	LiF(200)	Scint	Coarse	41.79	±0.40	100	100
Cu	Kα	LiF(200)	Scint	Coarse	45.02	±0.40	100	100
Ni	Kα	LiF(200)	Scint	Coarse	48.71	±0.60	100	100
Cr	Kα	LiF(200)	FPC	Fine	69.39	±0.50	100	100
Fe	Kα	LiF(220)	FPC	Fine	85.75	-0.40 + 0.70	40	40
V	Kα	LiF(220)	FPC	Fine	123.24	-0.50	100	60
TiO ₂	Kα	LiF(220)	FPC	Fine	86.17	±0.50	40	40
Ce	Lα	LiF(220)	FPC	Coarse	128.37	±1.50	100	100
Ba	Lβ	LiF(220)	FPC	Coarse	128.95	±1.50	100	100

Notes: Fe₂O₃* = total Fe as Fe₂O₃. FPC = flow proportional counter using P10 gas, KrSC = sealed krypton gas counter, and Scint = NaI scintillation counter. Elements analyzed under vacuum using goniometer 1 at generator settings of 60 kV and 50 mA.

formed and full of sediment across its entire diameter. The method is based on the attenuation, by Compton scattering, of a collimated beam of gamma rays passing through a known volume of sediment. This technique has been used for the measurement of sediment density since DSDP Leg 2 (Boyce, 1976). Measurements were made over 2-s windows, equivalent to a sample interval of 2.5 cm, while the core was moved with constant speed past the gamma-ray source and sensor. During Leg 144, the GRAPE was calibrated at least once every 24 hr by running an aluminum standard through the device. The GRAPE data were most reliable in APC cores.

Compressional Wave Velocity Logger

The compressional wave velocity logger, or *P*-wave logger (PWL), was operated simultaneously with the GRAPE and magnetic susceptibility meter on the MST. The PWL is designed to measure accurately the traveltime of an ultrasonic compressional pulse traveling through a sediment-filled plastic core liner. Spring-mounted acoustic transducers are positioned on either side of the core sections, thus making them parallel to the sediment bedding plane. The acoustic source produces a 500-kHz pulse at a repetition rate of 1000 Hz. The receiver detects the traveltime of the acoustic signal to an accuracy of 50 μs, which corresponds to an instrument resolution of 1.5 m/s for typical unlithified sediments recovered by the APC and XCB coring techniques.

The ultrasonic transducers were coupled with the plastic core liner by applying distilled water to their outer surface. Displacement transducers were used to monitor variations in liner diameter. The absolute accuracy of the measurement technique is estimated at 5 m/s because of variations in core liner thickness. The PWL was calibrated with a distilled water standard at least once per drill site. The sampling interval employed during Leg 144 was 5 cm. Generally, only the APC cores were measured. The data were edited on the basis of signal strength; all values below 30 were dropped. Problems associated with the transmission of the

acoustic pulse were often related to air gaps between the core and the plastic liner.

Magnetic Susceptibility

Magnetic susceptibility was measured on all core sections at 5-cm intervals using the 0.1 range on the Bartington meter with an 8-cm diameter loop. The close sampling was performed to provide another measure that could be used for between-hole correlation. Although the quality of these measurements degrades significantly in carbonate sediments, the general downhole trends can often be used for stratigraphic correlation (see "Paleomagnetism" section, this chapter). A MnO₂ standard was used to establish the calibration for this instrument.

Thermal Conductivity

The techniques used to measure thermal conductivity during Leg 144 are described in von Herzen and Maxwell (1959) for soft sediment and in Vacquier (1985) for hard rocks. All thermal conductivity data are reported in units of W/(m · K). For soft sediment, up to four needle probes were inserted into the core(s) through small holes drilled through the core liner. An additional needle was inserted in a standard. Once temperatures were stable, the probes were heated and the coefficient of thermal conductivity was calculated as a function of the change in resistance in the probe during each 20-s interval over a 6-min period. Sampled temperatures from the heating time interval (from 60 to 240 s) were fitted to the curve using a least-squares approximation as follows:

$$T(t) = F \cdot (q/4Qk) \cdot \ln(t) + A + Bt,$$

where

k = thermal conductivity,

T = temperature,

t = time since heater on,

q = heat input per unit length per unit time,

A and B = constant of a linear temperature drift, and

F = correction factor determined from the calibration tests made on standards before the measurement program.

Reliable measurements require that the temperature drift in the sample at the time of measurement be less than 4×10^{-2} °C/min. When the sediment became too stiff to allow easy insertion of the probe, holes were drilled into the core material before the probes were inserted. An attempt was made to insert the probes at locations along each core section that appear to be the least disturbed. However, an annulus of disturbed sediment and drill fluid was often present along the inside of the liner that prevented visual identification of the more intact segments in the core.

Hard-rock, split-core samples were measured for thermal conductivity determinations individually in a freshwater bath. A needle probe was sandwiched between a slab of low conducting material and the sample. The probe was heated, and measurements of resistance changes in the needle were made every 9 s over a 6-min period.

Compressional Wave Velocity

Compressional wave velocities were measured in soft sediments, such as unconsolidated to semiconsolidated pelagic ooze, using a Dalhousie University/Bedford Institute of Oceanography Digital Sound Velocimeter (DSV). Velocity calculations were based on the accurate measurement of the delay time of an impulsive acoustic signal traveling between a pair of piezoelectric transducers inserted in the split sediment cores. The transducers emit a 2- μ s square wave at about 250 and 750 kHz. A dedicated microcomputer controls all functions of the velocimeter. The transmitted and received signals are digitized by a Nicolet 320 digital oscilloscope and transferred to the microcomputer for processing. The DSV software selects the first arrival and calculates sediment velocity. The full waveform is stored for later calculation of attenuation.

Two acoustic transducers, positioned approximately 7 cm apart, were used to measure the vertical (along the core axis) compressional wave velocity. The transducers are firmly fixed at one end on a steel plate so that their separation does not change during velocity determinations. Periodically, the separation was precisely evaluated by running a calibration procedure in distilled water. Generally, the results of the velocity measurements in the unlithified pelagic ooze were very close to the P -wave velocity of seawater. On Leg 144, the APC coring apparently liquified the unstable sediment and therefore made the retrieved data unreliable. When coring disturbance seemed less likely, measurements were performed in the middle of every section. Where the sediment showed disturbance (liquefaction), no measurements were taken.

Discrete measurements of sonic velocity in lithified carbonate sediments and volcanic rocks were made using a Hamilton Frame velocimeter and a Tektronix Model DC 5010 counter/timer system. Velocities were calculated from the determination of the traveltime of a 500-kHz compressional wave through a measured thickness of sample. Discrete samples that were sufficiently competent to provide adequate signal strengths were used for these measurements. Rock samples were trimmed to a 2.5-cm cube with a double-bladed diamond core saw. Sampling density was largely dependent on rate of recovery and therefore was very irregular. Where core recovery and sample quality allowed, compressional wave velocity was analyzed in both the vertical and horizontal directions.

Zero traveltimes for the velocity transducers were estimated by linear regression of the traveltime vs. distance for a series of aluminum and lucite standards. The Nicolet 320 oscilloscope was

used to calculate velocities. Measurements were routinely made by propagating the waveform parallel to the core axis (longitudinal) and perpendicular to the split core surface (horizontal or transverse). This approach then provided a measure of the acoustic anisotropy within the sediment or rock. The anisotropy index was determined by the following relationship:

$$\text{Anisotropy} = 2(V_{pt} - V_{pl}) (V_{pt} + V_{pl})^{-1},$$

where V_{pt} is the transverse compressional wave velocity and V_{pl} the longitudinal velocity (Carlson and Christensen, 1977). Distilled water was used to improve the acoustic contact between the sample and the transducers. Velocities were not recorded when insufficient or extremely variable signals were obtained.

Shear Strength

The undrained shear strength of the sediment was determined using a Wykeham-Farrance (W-F) motorized vane apparatus, as described by Boyce (1977) and Lee (1984). A four-bladed vane with a 1:1 blade ratio and a dimension of 1.26 cm was used to make these measurements. The W-F vane apparatus has been modified so that greater speed and rotation can be achieved during testing.

The vane was inserted into the face of the split core section (perpendicular to the core axis), to a point where the top of the blade was covered by 4–6 mm of sediment. The vane was then rotated at a rate of about 90°/min until the sediment failed. The undrained shear strength was calculated from the peak torque observed at failure. The vane testing was suspended and the results rejected when radial cracking or other noncylindrical failure surfaces developed around the vane. In highly stiff, clayey sediments, a Soiltest torvane hand device with a high capacity CL-604 adapter was used to measure shear strength. The CL-604 adapter was inserted 3.4 mm deep into the split face of the core and carefully turned by hand. All shear strengths are reported in units of kilopascals (kPa). Calculations and calibration data were manipulated on the appropriate ODP Excell spreadsheets.

Index Properties

Index properties (wet- and dry-bulk density, grain density, water content, and porosity) were calculated from measurements of the wet and dry weights and volumes of discrete samples. Samples of approximately 10–20 cm³ were taken for determination of index properties. In addition, whole-core determinations of wet-bulk density were measured on the sediment using the gamma-ray attenuation porosity evaluator (GRAPE) on the MST.

Sample mass was determined aboard the ship to a precision of 0.03 g using a Scitech electronic balance. The sample mass was counterbalanced by a known mass such that only mass differentials of 0.5 g were measured. The balance is interfaced with a PRO-350 computer, which compensates for the motion of the ship by taking the average of a predetermined number of sample weighings (in this case equal to 500 times). Dry sample weight was determined using the same procedure after oven drying at 110°C for at least 24 hr and cooling in a desiccator. Sample volumes were determined using a Quantachrome Penta-Pycnometer, a helium-displacement pycnometer. The pycnometer measures volumes to a precision of ± 0.02 cm³. A reference volume was run with each group of samples during the first test series. Calibrations of the Penta-Pycnometer were conducted frequently during the cruise. Preliminary results suggest the pycnometer is fairly stable for a given cell inset, or sleeve; however, changing sleeves or insets offset the standard calibration by 0.1 cm³. The apparatus was used with small size beakers for soft sediments and the large inserts for hard-rock cubes.

Water Content

Determination of water content followed the methods of the American Society for Testing and Materials (ASTM) designation (D) 2216 (ASTM, 1989). As outlined in ASTM D 2216, corrections are required for salt when measuring marine samples. The index properties of unlithified sediment samples were corrected for salt. Hard-rock samples were placed in distilled water before being measured. The recommended equation for the water content calculation, which is the ratio of the pore-fluid mass to the dry sediment mass (% dry wt), is as follows:

$$W_c(\% \text{ dry wt}) = (M_t - M_d)/(M_d - rM_t) \cdot 100,$$

where

M_t = total mass (saturated),

M_d = dry mass, and

r = salinity (0.035).

Wet- and Dry-bulk Density

Wet-bulk density (ρ_w) is the density of the total sample including the pore fluid:

$$\rho_w (\text{g/cm}^3) = M_t/V_t$$

where V_t is the total sample volume. The mass (M_t) was measured using the electronic balance, and the total volume was measured with the helium pycnometer. Dry-bulk density (ρ_d), indispensable for calculating accumulation rates, is the dry mass per total (wet) volume:

$$\rho_d (\text{g/cm}^3) = M_d - r/(1 - r)(M_t - M_d)/V_t.$$

Porosity

Porosity values were calculated by means of the following equation:

$$\phi\% = (W_c \cdot \rho_w)/[(1 + W_c) \cdot \rho_f],$$

where

ρ_w is the wet-bulk density,

ρ_f is the density of the pore fluid (1.0245 g/cm³), and

W_c is the water content reported as a decimal ratio of % dry wt.

Grain Density

Grain density values were determined from the dry mass (Scitech balance) and dry volume (pycnometer) measurements. Both mass and volume were corrected for salt as follows:

$$\rho_{\text{grain}} (\text{g/cm}^3) = (M_d - s)/[V_d - (s/\rho_{\text{salt}})],$$

where

V_d = dry volume,

s = salt content (g) = $r/(1 - r)(M_t - M_d)$, and

ρ_{salt} = density of salt (2.257 g/cm³).

DOWNHOLE MEASUREMENTS

Logging Tool Strings

Downhole logs can be used to determine the physical and chemical properties of formations adjacent to the borehole. Interpretation of these continuous, in-situ measurements can yield a stratigraphic, lithologic, geophysical, and mineralogic characterization of the site. After coring is completed at a hole, a tool

string (a combination of several sensors) is lowered downhole on a seven-conductor cable, and each of the sensors in the tool string continuously monitors some property of the adjacent borehole. Although the depths of investigation are sensor dependent, data are typically recorded at 15-cm intervals. Four tool strings were used on Leg 144: the geophysical (quad-combo), Formation MicroScanner (FMS), and geochemical tool combinations of Schlumberger and a specialty tool—a slim-hole magnetometer. In addition, the Lamont-Doherty Geological Observatory temperature tool was attached to the base of the geophysical and geochemical tool strings to obtain heat-flow information. The slim-hole magnetometer was designed for use at sites with significant penetration into igneous basement.

The geophysical tool string used on Leg 144 consisted of the long-spaced sonic (LSS), natural gamma-ray tool (NGT), high-temperature lithodensity tool (HLDT), mechanical caliper (MCD), and an electrical resistance tool (phasor or dual induction tool; DITE) (Fig. 13). The NGT was run on each tool string to provide a basis for interlog correlations. The geophysical tool string measures compressional wave velocity and provides indicators of the two variables that most often control velocity: porosity, as indicated by density or resistivity; and clay content, as indicated by the natural gamma-ray spectrum from the NGT. The sonic velocity data, when combined with the information on density, were used to calculate an acoustic impedance log and generate a synthetic seismogram for the logged section.

The FMS tool string includes the Formation MicroScanner, the NGT, the MCD, and a general purpose inclinometer tool (GPIT), which spatially orients the Formation MicroScanner resistivity map of the borehole wall.

The geochemical combination string used on Leg 144 consists of the NGT, the aluminum clay tool (ACT), and the gamma spectrometry tool (GST) (Fig. 13). This tool combination measures the relative concentrations of silicon, calcium, aluminum, iron, sulfur, hydrogen, chlorine, potassium, thorium, and uranium.

Logging Tools

A brief description of logging tools run during Leg 144 is given in the following section. A detailed description of logging tool principles and applications is provided in Schlumberger (1972), Serra (1984), and Timur and Toksoz (1985).

Electrical Resistivity Tool

The phasor or dual induction tool (DITE) provides three different measurements of electrical resistivity, each one with a different depth of investigation. Two induction devices (deep- and medium-penetration resistivity) send high-frequency alternating currents through transmitter coils, creating magnetic fields that induce secondary (Foucault) currents in the formation (Fig. 14A). These ground-loop currents produce new inductive signals, proportional to the conductivity of the formation, which are recorded by the receiving coils. Measured conductivities then are converted to resistivity. A third device (spherically focused resistivity; Fig. 14B) measures the current necessary to maintain a constant voltage drop across a fixed interval. Vertical resolution is around 150 cm for the medium-penetration device, 200 cm for the deep-penetration resistivity device, and about 75 cm for the spherically focused resistivity device.

Water content and salinity are by far the most important factors controlling the electrical resistivity of rocks. To the first order, resistivity is proportional to the inverse square root of porosity (Archie, 1942). Other factors influencing resistivity include the concentration of hydrous and metallic minerals, vesicularity, and geometry of interconnected pore space.

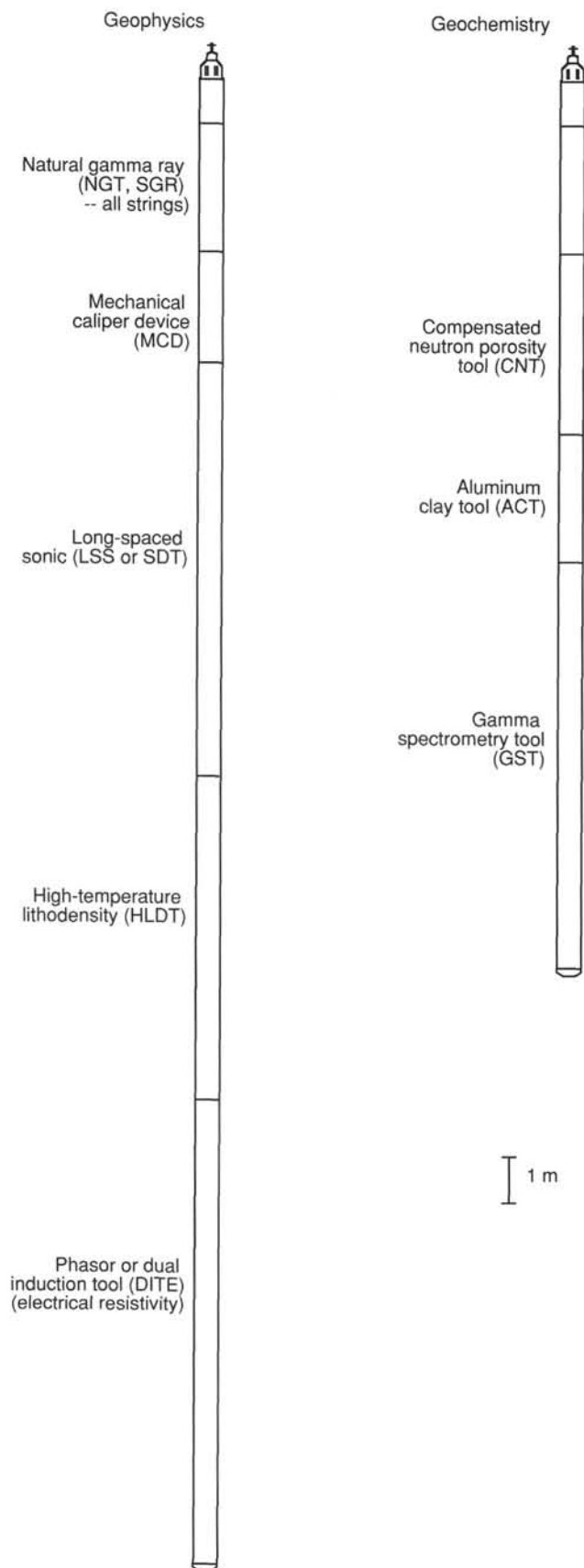


Figure 13. Schematics of geophysical and geochemical logging tool strings.

Sonic Velocity Tool

The long-spaced sonic (LSS) tool uses two acoustic transmitters and two receivers to measure the time required for sound waves to travel over source-receiver distances of 2.4, 3.0, and 3.6 m (Fig. 15). The raw data are reported as the time required for a sound wave to travel through 0.31 m of formation; these traveltimes are then converted to sonic velocities. First arrivals for the individual source-receiver paths are used to calculate the velocities of the different waves traveling in the formation (compressional, shear, etc.). Only compressional wave velocity is determined during data acquisition, but waveforms are recorded for post-cruise determination of shear-wave velocities and possibly improved compressional wave velocities. The vertical resolution of the tool is 60 cm. Compressional wave velocity is dominantly controlled by porosity and degree of lithification; this velocity increases with either a decrease in porosity or an increase in lithification.

Lithodensity Tool

The high-temperature lithodensity tool (HLDT) measures the energy flux at fixed distances from the Cesium-137 (^{137}Ce) gamma-ray source (Fig. 16). Under normal operating conditions, attenuation of gamma rays is caused chiefly by Compton scattering (Dewen, 1983). Formation density is extrapolated from this energy flux by assuming that the atomic weight of most rock-forming elements is approximately twice the atomic number. A photoelectric-effect index is also provided. Photoelectric absorption occurs in the energy window below 150 keV and depends on the energy of the incident gamma ray, the atomic cross section, and the nature of the atom. Because this measurement is almost independent of porosity, it can be used directly as an indicator of matrix lithology.

The radioactive source and detector array are placed in a tool that is pressed against the borehole wall by a strong spring arm; the position of this spring arm relative to the tool indicates hole diameter. Excessive roughness of the hole will cause some drilling fluid to infiltrate between the detector and the formation. As a consequence, density readings can be artificially low. Approximate corrections can be applied by using caliper data. The vertical resolution is about 38 cm.

Natural Gamma-ray Tool

The natural gamma-ray tool (NGT) measures the natural radioactivity of the formation. Most gamma rays are emitted by the radioactive isotope of potassium (^{40}K) and by the radioactive elements of the uranium (U) and thorium (Th) series. The gamma-ray radiation originating in the formation close to the borehole wall is measured by a scintillation detector mounted inside the tool. Measurements are analyzed by subdividing the entire incident gamma-ray spectrum into five discrete energy windows. The total counts recorded in each window, for a specified depth in the well, are processed to give the elemental abundances of K, U, and Th. The final outputs are the total gamma ray (SGR), a uranium-free gamma-ray measurement (CGR), and the concentrations of potassium (in weight % or decimal fraction), thorium (ppm), and uranium (ppm). The vertical resolution of the log is about 50 cm.

Because radioactive elements tend to be most abundant in clay minerals, the gamma-ray curve is commonly used to estimate the clay or shale content. There are rock matrices, however, for which the radioactivity ranges from moderate to extremely high values as a result of the presence of volcanic ash, potassic feldspar, or other radioactive minerals.

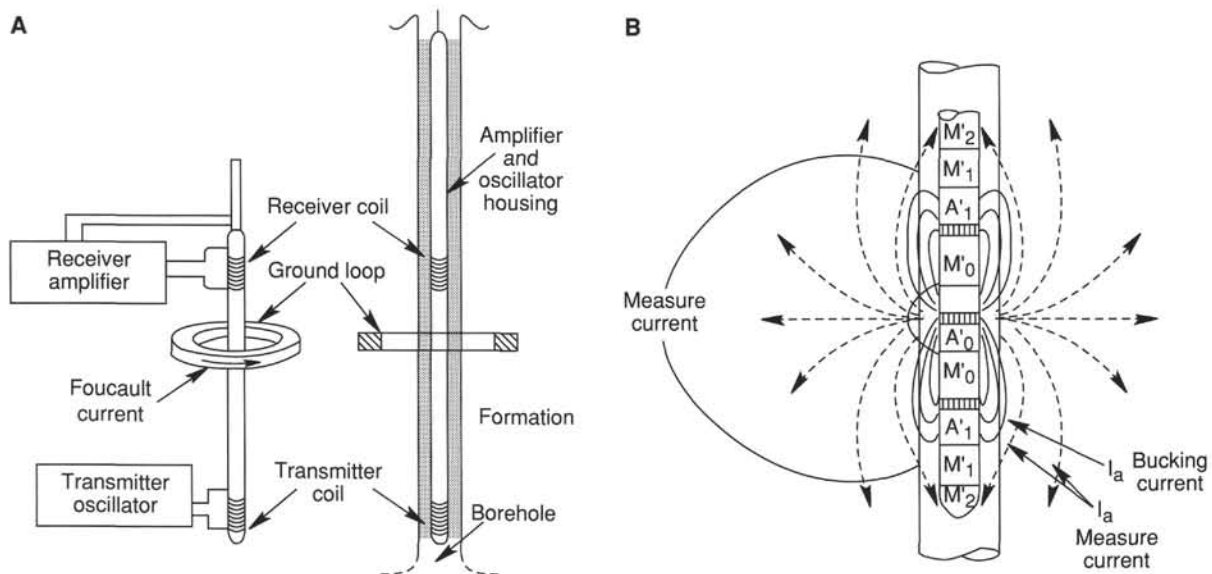


Figure 14. Sketch of Schlumberger resistivity devices used in the Ocean Drilling Program. A. Phasor induction tool (DITE). B. Spherically focused resistivity tool (SFL).

Gamma Spectrometry Tool

The induced spectral gamma-ray tool (GST) consists of a pulsed source of 14-MeV neutrons and a gamma-ray scintillation detector. A shipboard computer performs spectral analysis of gamma rays generated by the interactions of neutrons emitted by the source with atomic nuclei in the formation (Hertzog, 1979). Characteristic sets of gamma rays from six elements dominate the spectrum, permitting calculation of six elemental yields: calcium, silicon, iron, sulfur, chlorine, and hydrogen (Ca, Si, Fe, S, Cl, and H). The tool normalizes their sum, so that the yields do not reflect the actual elemental composition. Instead, ratios of these elemental yields are commonly used in interpreting lithologic characteristics, porosity, and the salinity of the formation fluid. Shore-based processing is used to compute new elemental yields and the absolute dry-weight fractions of the major oxides.

Aluminum Clay Tool

Aluminum (Al) abundance as measured by the aluminum clay tool (ACT) is determined by neutron-induced, late-arrival, gamma-ray spectrometry using californium as the chemical source. By placing NGT tools, which contain sodium-iodide (NaI) detectors, above and below the neutron source, contributions from natural gamma-ray activity can be removed.

Calibration to elemental weight percent is performed by taking irradiated core samples of known volume and density and measuring their gamma-ray output while being placed in a jig attached to the logging tool (generally after logging).

Formation MicroScanner

The Formation MicroScanner (FMS) produces high-resolution microresistivity images of the borehole wall that can be used for detailed sedimentological or structural interpretations, and for determining fracture and breakout orientations. The tool (Fig. 17) consists of 16 electrodes, or "buttons," on each of 4 orthogonal pads that are pressed against the borehole wall. The electrodes are spaced about 2.5 mm apart and are arranged in 2 diagonally offset rows of 8 electrodes each. The focused current that flows from the buttons is recorded as a series of curves that reflect the microresistivity variations of the formation. Onboard or shore-based processing converts the measurements into complete, spa-

tially oriented images of the borehole wall. Further processing can provide measurements of dip and direction or azimuth of planar features. The vertical resolution of the FMS is about 2 cm, but coverage is restricted to about 22% of the borehole wall for each pass of the tool.

Applications of the FMS images include detailed correlation of coring and logging depths, orientation of cores, and mapping of fractures, faults, foliations and formation structures, as well as the determination of strikes and dips of bedding. An important limitation of the tool is the restriction of hole diameter to <37 cm (14.5 in.). Thus, no useful information can be obtained from washed-out hole sections.

In addition to imaging structures within the borehole, the four groups of resistance traces can be cross-correlated to provide measurements of dip direction and angle of beds and fractures.

General Purpose Inclinometer Tool

This inclinometer tool (GPIT) provides measurements of the deviation of the borehole from vertical, the orientation of the tool with respect to the Earth's magnetic field using a three-component magnetometer, and the tool motion using an accelerometer. It is run with the FMS to provide spatial orientation for the borehole wall images. In basement sections of the borehole, tool orientation is not possible on account of the local magnetic anomalies generated by the high remanent magnetization of basalts. However, these magnetic anomalies can be used instead to infer the magnetic polarity stratigraphy of the basement section.

Mechanical Caliper Device

The mechanical caliper device (MCD) provides a measure of borehole diameter. The hole-diameter log is used to detect wash-outs or constrictions. Borehole diameter significantly affects many of the other logging measurements, and the hole diameter is an important input to log correction routines. This caliper tool is subject to sticking when formation mud gets into its mechanical parts, resulting in bimodal (fully open or nearly fully closed) readings. In contrast, the hole-diameter measurement produced by the high-temperature lithodensity tool is much more reliable. Consequently, on Leg 144 the MCD tool was used primarily to provide centralization and associated improved log quality for the sonic log rather than to measure hole diameter.

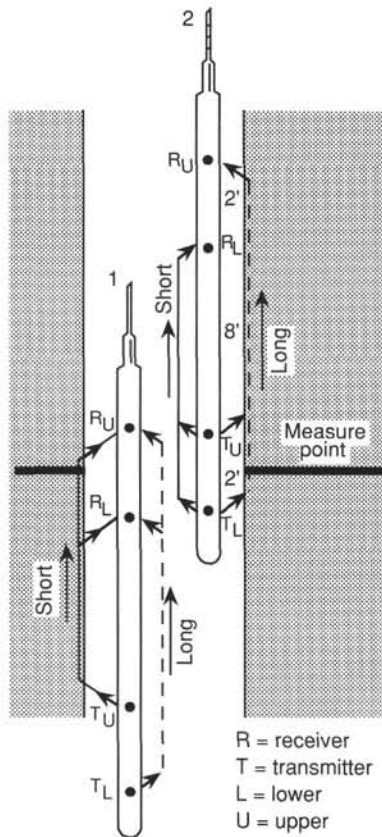


Figure 15. Sketch of the Schlumberger acoustic tool (long spacing sonic [LSS]) illustrating how a particular interval (measure point) would first (1) be measured by the acoustic paths from the T_U transmitter to the R_U and R_L receivers, and then (2) by the acoustic paths from the T_L transmitter to the R_U and R_L receivers. Four delay times are averaged to calculate acoustic velocity at the measure point.

The mechanical calipers, when run simultaneously with the general purpose inclinometer tool on the FMS string, can also be used to measure orientations of in-situ stress by using breakout locations. In an isotropic, linearly elastic rock subjected to an isotropic stress field, breakouts form in the direction of the least principal horizontal stress. Bell and Gough (1979) and Zoback et al. (1988) demonstrated that the stress orientations deduced from such rock breakouts are consistent with other independent stress indicators.

Temperature Tool of Lamont-Doherty

The Lamont-Doherty temperature tool (LTL) is a self-contained tool that can be attached to any Schlumberger tool string. Data from two thermistors and a pressure transducer are collected at a predetermined rate, between 0.5 and 5.0 s, and stored in a Tattletale computer within the tool. Following the logging run, data are transferred from the Tattletale to a shipboard computer for analysis. A fast-response, lower accuracy thermistor is able to detect sudden, very small temperature excursions caused by fluid flow from the formation. A slow-response, higher accuracy thermistor can be used to estimate heat flow, provided the history of drilling-fluid circulation in the hole and at least two temperature logs are available (Jaeger, 1961). Data are recorded as a function of time; conversion to depth can be based on the pressure transducer or, preferably, on simultaneous recording by Schlumberger of both depth and time.

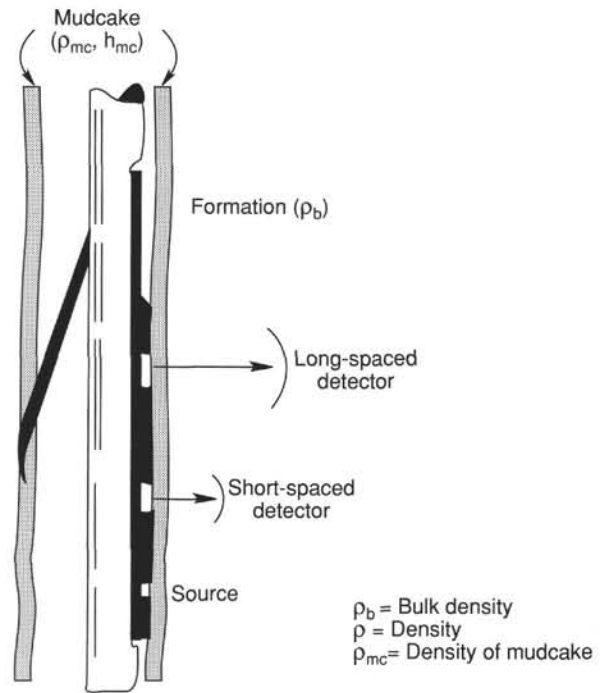


Figure 16. Schematic drawing of Schlumberger high-temperature lithodensity (HLDT) tool used in the Ocean Drilling Program to measure density and porosity.

Three-component Magnetometer

This downhole magnetometer was designed and fabricated in Japan for downhole measurements in ODP holes. The cylindrical magnetometer is 4.6 m long and 6.7 cm in diameter, which enables its use in almost all DSDP and ODP holes. The magnetometer measuring units are housed within high-pressure vessels made of MONEL alloy (Fig. 18). This nonmagnetic MONEL alloy (magnetic permeability is 1.001) retains high tensile strength at high temperatures (no deterioration of strength up to 650°C). For ease of transport, the pressure vessel is separated into four sections: (1) sensors, (2) electronics, (3) batteries, and (4) weights. The length of each section is about 1.2 m. For downhole operations, these four sections are connected into one long cylinder with rubber O-rings providing water-tight seals. The total weight of the magnetometer tool is about 100 kg.

This downhole magnetometer measures the three orthogonal components of the magnetic field and records internal temperature. Ring-core fluxgate-type magnetic sensors are used for detecting the magnetic field (Fig. 19). Three mutually perpendicular ring cores, drive coils, and pick-up coils are installed in the bottom section of the magnetometer. A semiconductor temperature sensor (AD590) is placed close to the fluxgate sensor. The fluxgate and temperature sensors are installed near the lower end of the bottom section.

The second section of the magnetometer houses electronics for the fluxgate magnetometer and temperature sensors, an analog-to-digital (A/D) converter, and an integrated-circuit (IC) memory. The fluxgate magnetometer electronics consist of the driving and the detection circuitry for the magnetic sensor. The driving frequency of the fluxgate sensor is 15 kHz, and the detection circuit converts the amplitude of higher harmonics, which is proportional to the external field strength in the sensor detection, to the direct-current (DC) output voltage. The sixteen-bit A/D converter is used by the three magnetic sensors and the temperature sensor.

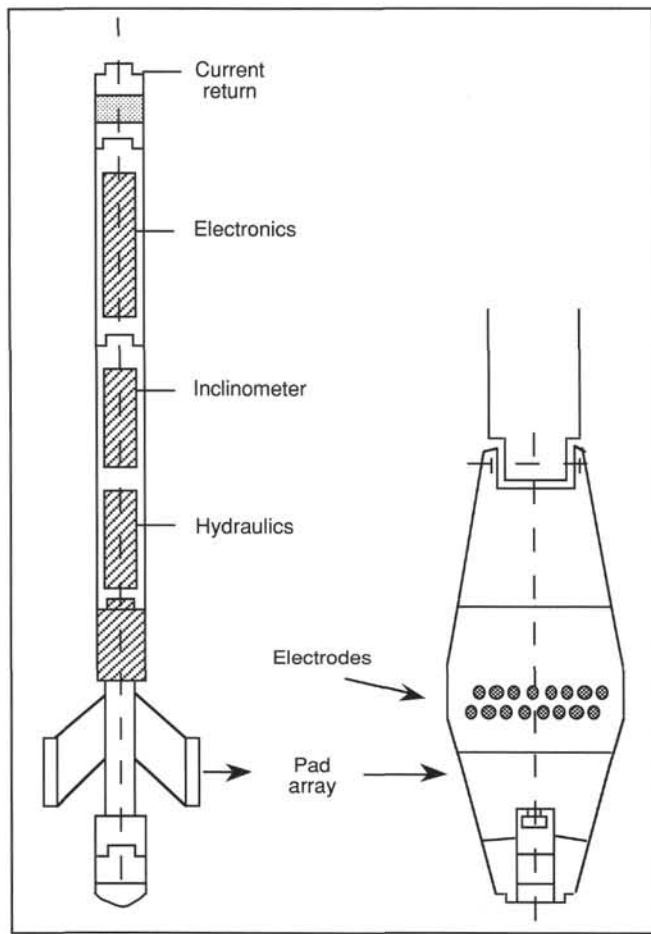


Figure 17. Formation MicroScanner (FMS) resistivity logging tool. Four pads, each containing a grid of electrodes spaced at approximately 2.5-mm intervals, provide a continuous record of resistivity of the borehole walls. Additional instruments in the FMS tool string are an inclinometer and magnetometer to measure orientation of the traces, an accelerometer to convert the time record to a depth record of microresistivity, and a dipmeter array to measure structural attitudes. The tool string is about 6 m long. Sketch modified from Pezard et al. (1990).

The digital data signals from the A/D converters are stored in IC memory, consisting of electrically programmable read-only memory (EPROM). The maximum available memory space is 2 Mb.

The third section contains a battery power source for the magnetometer. Seven lithium batteries (National BR-C) are used to supply a voltage of ± 18 V. The uppermost section contains lead weights, which increase the total mass for deployment purposes.

Besides the magnetometer, an on-board controller box is provided. This box gives external power to check the magnetometer operation and transmits control signals to the magnetometer. This box also contains an interface for the transfer of data from the magnetometer to a microcomputer for permanent storage. An NEC PC-9801 compatible computer is used as a host computer.

Resolution of the magnetic field is changeable; settings are 1.02, 1.36, and 2.03 nannoteslas (nT). These resolution settings were calibrated by a Helmholtz coil at the Kakioka Magnetic Observatory of Japan Meteorological Agency (JMA). The measurement range of the magnetic field of each axis of the magnetometer is ± 66519 nT for lower resolution. The sampling interval is 3 s, and the maximum operation time is 12 hr.

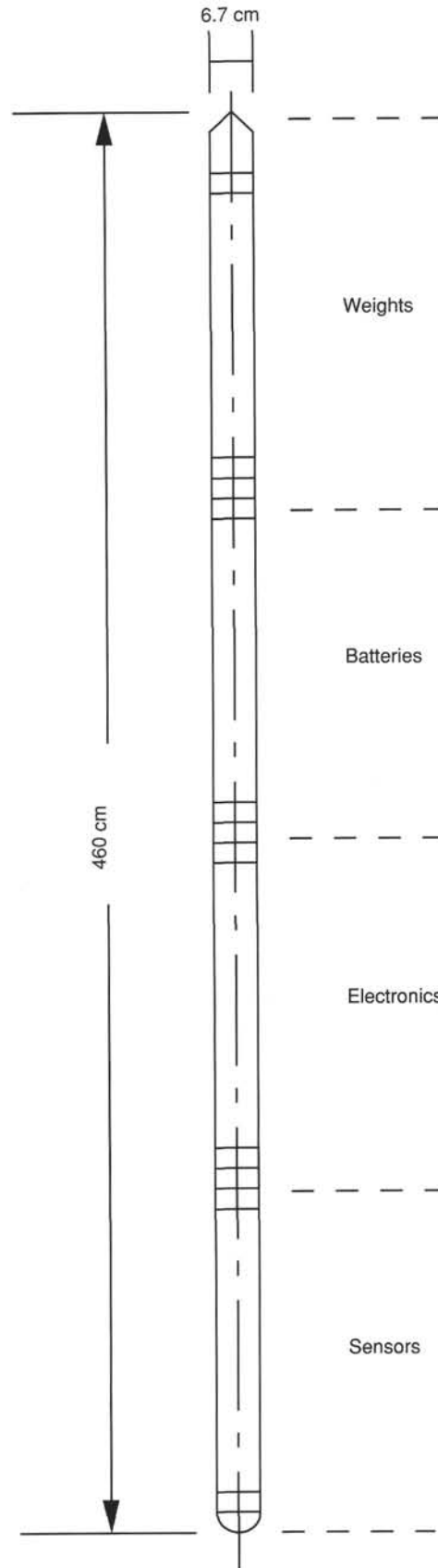


Figure 18. Schematic drawing of the downhole magnetometer tool.

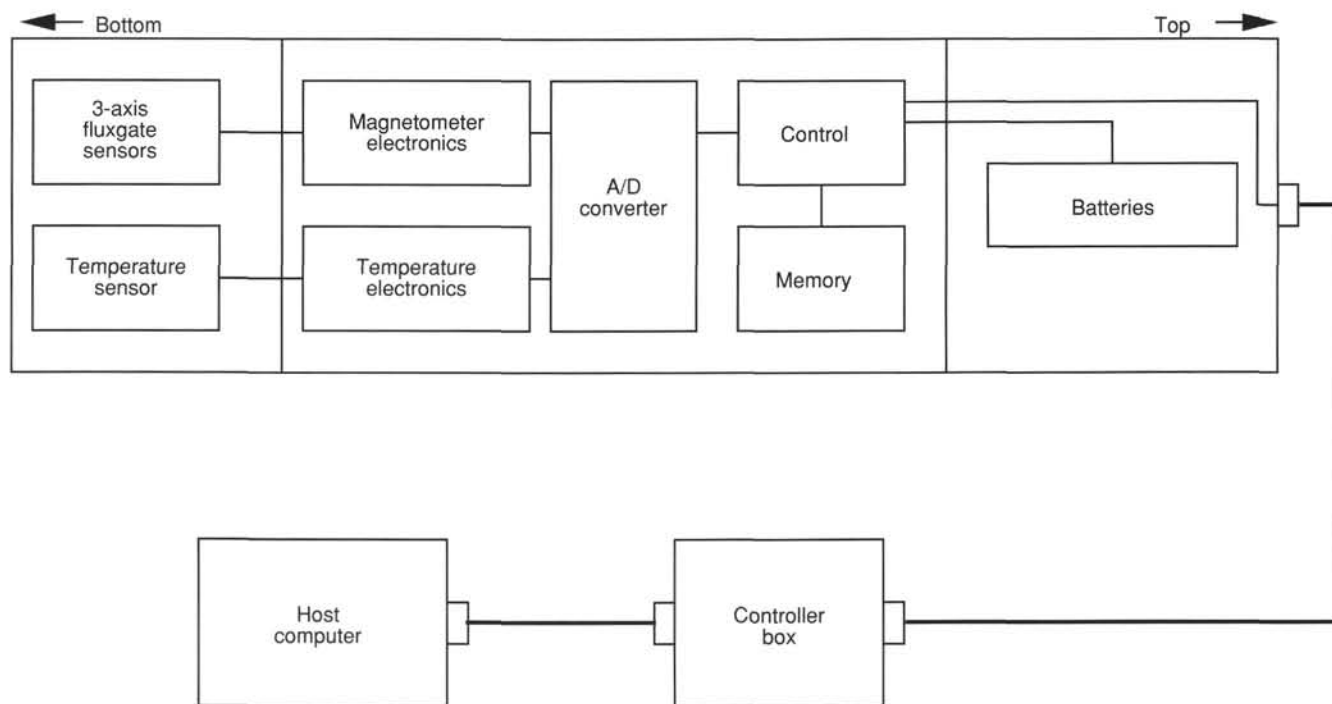


Figure 19. Downhole magnetometer electronics in block-diagram form.

Wireline Packer

The wireline packer, designed and built by TAM International, is a discrete-zone, pore-fluid sampler. This tool was used only within the Jurassic basaltic crust in Hole 801C. The tool is run by means of a standard seven-conductor logging cable. Unlike a drill-string packer, which is actuated by dropping a go-devil and pumping through the pipe, the wireline packer is controlled by a surface computer in either the winch room or the downhole measurements laboratory. No hydraulic connection with the surface is required, as the tool contains an electrically operated, downhole pumping system. The wireline packer is a straddle tool, meaning that it has two distinct inflation elements. When inflated, the elements isolate a vertical zone approximately 1 m in length from which fluid can be extracted.

Because it must pass through the drill pipe and the bottom-hole assembly (BHA), the outer diameter of the packer is limited by the 9.65-cm inner diameter of standard ODP bottom-hole assemblies. The two packer elements will inflate to a maximum of 30.5 cm (12 in.) at a pressure of about 350 psi differential. Differential pressure is kept relatively low to prevent rupturing of the bladders in the packer elements, which are strained by high expansion.

Following packer inflation, fluid is drawn from the interval isolated by the packer elements and pumped out to the annulus. The pump has an output of approximately 5 L/min and a maximum drawdown of about 350 psi. Actual pump rates and zone pressures are controlled by the permeability of the formation. Zone and packer pressures, temperature, and fluid chemistry (sodium, calcium, and chloride concentrations and pH) are continuously monitored and digitally transmitted to the surface.

By monitoring the geochemical data in real time, the operator can determine when a reasonable concentration of pristine formation fluid is present in the system, and redirect fluid flow into one of four sampling bottles. The sampling bottles are similar in design to a syringe, each having a capacity of about 400 mL. Each bottle is equipped with a check valve to maintain fluid pressure following sampling. Once a sample is collected, the packers can

be deflated and the tool moved to a new location. At the completion of the sampling program, the tool is drawn back up inside the bit and returned to the surface, where the samples are removed for analysis.

Log Data Quality

The quality of log data may be seriously degraded by excessively wide sections of the borehole or by rapid changes in the hole diameter. Resistivity and velocity measurements are least sensitive to borehole effects, whereas the nuclear measurements (density, neutron porosity, and both natural and induced spectral gamma ray) are most sensitive because of the large attenuation by the borehole fluid. Corrections can be applied to the original data to reduce the effects of these conditions and, generally, any departure from the conditions under which the tool was calibrated.

Logs from different tool strings may have small depth mismatches, caused by either cable stretch or ship heave during recording. Small errors in depth matching can impair the logging results in zones of rapidly varying lithology. To minimize the effects of ship heave, a hydraulic heave compensator adjusts for rig motion during logging operations. Distinctive features recorded by the natural gamma tool (NGT), run on every log tool string, provide correlation and relative depth offsets among the logging runs and can be calibrated to distinctive lithologic contacts observed in the core recovery or drilling penetration (e.g., basement contacts). Precise depth matching of logs with cores is difficult in zones where core recovery is low because of the inherent ambiguity of placing the recovered section within the cored interval.

Log Analysis

During logging, incoming data are observed on a monitor oscilloscope and simultaneously recorded on digital tape in the Schlumberger logging unit. After logging, the Schlumberger tape was read by computer in the downhole measurements laboratory and reformatted to a file format (LIS) compatible with the Terralog log-interpretation software package. Terralog is an interac-

tive system consisting of many log manipulation and plot options. Additional logging interpretations and plotting were accomplished by conversion to ASCII text files, which were transferred to Macintosh-PC spreadsheet and graphics packages. Most log interpretation was conducted aboard ship; further processing and interpretation were undertaken after the cruise at the Borehole Research Laboratory of Lamont-Doherty Geological Observatory.

Synthetic Seismograms

Synthetic seismograms are generated from logging velocity data obtained with the long-spaced sonic (LSS) tool. The bulk density log from the lithodensity tool or a pseudodensity log created from other logs is required in addition to the LSS log. In many cases, a simple constant density log can be assumed. Experience shows that this often gives accurate results, because both velocity and density are usually controlled by the same parameter: porosity. When velocity and density are highly correlated, synthetic seismograms using either a constant density log or an actual density log are virtually identical.

The slowness and density logs are used in a computer program that generates an acoustic impedance log (velocity \times density), which is convolved with a zero-phase Ricker or other assumed wavelet. The frequency of this wavelet can be varied depending on the source that generated the original seismic profile. A 30-Hz wavelet is capable of a vertical resolution on the order of 30 m, so reflectors cannot generally be attributed to any small-scale lithologic horizons. The synthetic seismogram is calculated based on a convolutional model, with interbed multiples.

Sonic logs obtained in real time are not based on full-waveform analysis, but on a thresholding technique that attempts to detect the compressional wave arrival by a first-break criterion. Occasionally, this technique fails and either the threshold is exceeded by noise or the first compressional arrival is below the threshold. This phenomenon, called cycle skipping, creates spurious spikes on the sonic log. On Leg 144, raw traveltimes were reprocessed with an algorithm designed to reject cycle skips (Shipboard Scientific Party, 1987).

Reprocessing of Geochemical Logs

Raw count rates for six elements (Ca, Si, Fe, S, Cl, and H) are obtained in real time by the Schlumberger data acquisition software. Post-cruise reprocessing, using a Schlumberger Elite 1000 workstation, proprietary Schlumberger software, and a revised algorithm, inverts the gamma spectrum at each depth for titanium, gadolinium, and potassium in addition to the six elements (Ca, Si, Fe, S, Cl, and H) in the shipboard inversion. Though gadolinium is present in concentrations of only a few parts per million, its neutron capture cross section is so large that gadolinium can account for 10%–30% of the total gamma spectrum. Inclusion of these additional elements improves the quality of the overall inversion, particularly improving the accuracy of calculated calcium abundance by converting sources of unaccounted variance to signals. However, the determined potassium concentrations are less accurate than those from the NGT, and the hydrogen concentrations are less accurate than those from the neutron tool.

When both the geophysical and geochemical Schlumberger tool strings are run, further reprocessing of geochemical logs is possible. The relative abundances of Ca, Si, Fe, Ti, Al, K, S, Th, U, and Gd are used to calculate a log of predicted photoelectric effect. The difference between this log and the actual log of photoelectric effect can be attributed to the only two major elements not directly measured, Mg and Na. Major elements are converted from volume percent to weight percent using logs of total porosity (bound water plus pore water) and density. Major elements are expressed in terms of oxide dry weight percent,

based on the assumption that oxygen is 50% of the total dry weight.

If geochemical tool string data are available but not enough log types are run to permit complete solution for oxide weight percentage, one further processing step is made. Omitting chlorine and hydrogen, the yields of the other geochemical-tool elements (Ca, Si, Fe, Ti, S, K, and Gd) are summed, and each is expressed as a fraction of this total yield. This procedure corrects for porosity and count rate variations. Although the absolute abundance of each element is not determined, downhole variations in relative abundance are indicated.

Core-log Integration

The precision and reliability of the various logging measurements are governed by the resolution of the various tools and the condition of the drill hole. Vertical resolutions by the various logging tools generally range from 50 to 60 cm, except for the medium and deep resistivity tools, which have 1.5 and 2 m resolutions, respectively, and the Formation MicroScanner tool, which has a resolution of 0.5–1.0 cm. The data were collected at 15-cm (0.50-ft) intervals, except for the Formation MicroScanner runs, which were sampled at a rate of 2.5 mm (0.10 in.).

Core-log integration on Leg 144 involved comparing recovered lithologies in cores with the corresponding responses of the various logs within the drilled intervals. After calibrating the logs with the core recovery on a small scale, the logs can then be used to interpret details of the sequences that were not recovered during coring.

The primary logging tools used in the core-to-log integration were the Formation MicroScanner high-resolution microresistivity imagery of the hole, the natural gamma-ray spectrum, the lithodensity log, and the geochemical logs. These selected logs were simultaneously displayed using a common 1:40 scale and were compared to the corresponding core photographs and visual descriptions. The resolution and interpretation of sedimentary structures was accomplished using a 1:6 scale of images taken with the Formation MicroScanner and comparing them to core closeup photographs and visual descriptions.

REFERENCES*

- Archie, G.E., 1942. The electrical resistivity log as an aid in determining some reservoir characteristics. *J. Pet. Technol.*, 5:1–8.
- Arnaut, A., Berthou, P.Y., Brun, L., Cherchi, A., Chiochini, M., De Castro, P., Fourcade, E., Garcia Quintane, A., Hamaoui, M., Lamolda, M., Luperto Sinni, E., Neumann, M., Prestat, B., Schroeder, R., and Tronchetti, G., 1981. Tableau de répartition stratigraphique des grands foraminifères caractéristiques du Crétacé moyen de la région méditerranéenne. *Cretaceous Res.*, 2:383–393.
- ASTM, 1989. Annual Book of ASTM Standards for Soil and Rock, Building Stones: *Geotextiles*. 0408: Philadelphia (Am. Soc. for Testing and Materials).
- Barron, J.A., 1985. Miocene to Holocene planktic diatoms. In Bolli, H.M., Saunders, J.A., and Perch-Nielsen, K. (Eds.), *Plankton Stratigraphy*: Cambridge (Cambridge Univ. Press), 763–809.
- Bell, J.S., and Gough, D.I., 1979. Northeast-southwest compressive stress in Alberta: evidence from oil wells. *Earth Planet. Sci. Lett.*, 45:475–482.
- Berggren, W.A., Kent, D.V., and Flynn, J.J., 1985. Jurassic to Paleogene: Part 2. Paleogene geochronology and chronostratigraphy. In Snelling, N.J. (Ed.), *The Chronology of the Geologic Record*. Geol. Soc. London Mem., 10:141–195.
- Berggren, W.A., Kent, D.V., Flynn, J.J., and van Couvering, J.A., 1985. Cenozoic geochronology. *Geol. Soc. Am. Bull.*, 96:1407–1418.
- Berggren, W.A., Kent, D.V., and van Couvering, J.A., 1985. The Neogene: Part 2. Neogene geochronology and chronostratigraphy. In

* Abbreviations for names of organizations and publication titles in ODP reference lists follow the style given in *Chemical Abstracts Service Source Index* (published by American Chemical Society).

- Snelling, N.J. (Ed.), *The Chronology of the Geologic Record*. Geol. Soc. London Mem., 10:211–260.
- Berggren, W.A., and Miller, K.G., 1988. Paleogene tropical planktonic foraminiferal biostratigraphy and magnetostratigraphy. *Micropaleontology*, 34:362–380.
- Blow, W.H., 1969. Late middle Eocene to Recent planktonic foraminiferal biostratigraphy. In Brönnimann, P., and Renz, H.H. (Eds.), *Proceedings of the First International Conference on Planktonic Microfossils, Geneva, 1967*: Leiden (E.J. Brill), 1:199–422.
- Boyce, R.E., 1976. Definitions and laboratory techniques of compressional sound velocity parameters and wet-water content, wet-bulk density, and porosity parameters by gravimetric and gamma ray attenuation techniques. In Schlanger, S.O., Jackson, E.D., et al., *Init. Repts. DSDP*, 33: Washington (U.S. Govt. Printing Office), 931–958.
- , 1977. Deep Sea Drilling Project procedures for shear strength measurements of clayey sediment using modified Wykeham-Farrance laboratory apparatus. In Barker, P.E., Dalziel, I.W.D., et al., *Init. Repts. DSDP*, 36: Washington (U.S. Govt. Printing Office), 1059–1068.
- Bralower, T.J., 1987. Valanginian to Aptian calcareous nannofossil stratigraphy and correlation with the upper M-sequence magnetic anomalies. *Mar. Micropaleontol.*, 11:293–310.
- Bukry, D., 1973. Low latitude coccolith biostratigraphic zonation. In Edgar, N.T., Saunders, J.B., et al., 1973, *Init. Repts. DSDP*, 15: Washington (U.S. Govt. Printing Office), 685–703.
- , 1975. Coccolith and silicoflagellate stratigraphy, northwestern Pacific Ocean, Deep Sea Drilling Project Leg 32. In Larson, R.L., Moberly, R., et al., *Init. Repts. DSDP*, 32: Washington (U.S. Govt. Printing Office), 677–701.
- Burckle, L.H., 1972. Late Cenozoic planktonic diatom zones from the eastern equatorial Pacific. *Nova Hedwigia*, 39:217–246.
- Carlson, R.L., and Christensen, N.I., 1977. Velocity anisotropy and physical properties of deep-sea sediments from the western South Atlantic. In Perch-Nielsen, K., Supko, P.R., et al., *Init. Repts. DSDP*, 39: Washington (U.S. Govt. Printing Office), 555–559.
- Caron, M., 1985. Cretaceous planktic foraminifera. In Bolli, H.M., Saunders, J.B., and Perch-Nielsen, K. (Eds.), *Plankton Stratigraphy*: Cambridge (Cambridge University Press), 17–86.
- Channell, J.E.T., and Erba, E., 1992. Early Cretaceous polarity Chrons CMO to CMI 1 recorded in northern Italian land sections near Brescia (Northern Italy). *Earth. Planet. Sci. Lett.*, 108:161–179.
- Choquette, P.W., and Pray, L.C., 1970. Geological nomenclature and classification of porosity in sedimentary carbonates. *AAPG Bull.*, 54:207–250.
- Coccioni, R., Erba, E., and Premoli Silva, I., 1992. Barremian-Aptian calcareous plankton biostratigraphy from the Gorgo Cerbara section (Marche, central Italy) and implications for plankton evolution. *Cretaceous Res.*, 13.
- Damassa, S.P., Goodman, D.K., Kidson, E.J., and Williams, G.L., 1990. Correlation of Paleogene dinoflagellate assemblages to standard nannofossil zonation in North Atlantic DSDP sites. *Rev. Paleobot. Palynol.*, 65:331–339.
- Davies, P., McKenzie, J.A., Palmer-Julson, A., et al., 1991. *Proc. ODP, Init. Repts.*, 133: College Station, TX (Ocean Drilling Program).
- De Vernal, A., and Mudie, P.J., 1989a. Pliocene and Pleistocene palynostratigraphy at ODP Sites 646 and 647, eastern and southern Labrador Sea. In Srivastava, S.P., Arthur, M., Clement, B., et al., *Proc. ODP, Sci. Results*, 105: College Station, TX (Ocean Drilling Program), 401–422.
- , 1989b. Late Pliocene to Holocene palynostratigraphy at ODP Site 645, Baffin Bay. In Srivastava, S.P., Arthur, M., Clement, B., et al., *Proc. ODP, Sci. Results*, 105: College Station, TX (Ocean Drilling Program), 387–399.
- Dewen, J.T., 1983. *Essentials of Modern Open Hole Log Interpretations*: Tulsa (Penwall).
- Dunham, R., 1962. Classification of carbonate rocks according to depositional texture. In Ham, W.E. (Ed.), *Classification of Carbonate Rocks*. AAPG Mem., 108–121.
- Embry, A.F., and Klovan, J.E., 1971. A late Devonian reef tract on northeastern Banks Island, Northwest Territories. *Bull. Can. Pet. Geol.*, 19:730–781.
- Emeis, K.C., and Kvenvolden, K.A., 1986. *Shipboard Organic Geochemistry on JOIDES Resolution*. ODP Tech. Note, 7.
- Espitalié, J., Deroo, G., and Marqui, F., 1985a. La pyrolyse Rock-Eval et ses applications. *Rev. Inst. Fr. Petr.*, 40:563–579.
- , 1985b. La pyrolyse Rock-Eval et ses applications. *Rev. Inst. Fr. Petr.*, 40:755–784.
- , 1986. La pyrolyse Rock-Eval et ses applications. *Rev. Inst. Fr. Petr.*, 41:73–89.
- Fisher, R.V., and Schmincke, H.U., 1984. *Pyroclastic Rocks*: Berlin (Springer-Verlag).
- Folk, R.L., 1965. Some aspects of recrystallization in ancient limestones. In Pray, L.C., and Murray, R.C. (Eds.), *Dolomitization and Limestone Diagenesis*. Spec. Publ.—Soc. Econ. Paleontol. Mineral., 13:13–48.
- Gartner, S., 1977. Calcareous nannofossil biostratigraphy and revised zonation of the Pleistocene. *Mar. Micropaleontol.*, 2:1–25.
- Gealy, J.M., Winterer, E.L., and Moberly, R., 1971. Methods, conventions and general observations. In Winterer, E.L., Riedel, W.R., et al., *Init. Repts. DSDP*, 7 (Pt. 1): Washington (U.S. Govt. Printing Office), 9–26.
- Gieskes, J.M., Gamo, T., and Brumsack, H., 1991. *Chemical Methods for Interstitial Water Analysis Aboard JOIDES Resolution*. ODP Tech. Note, 15.
- Harland, W.B., Armstrong, R.L., Cox, A.V., Craig, L.E., Smith, A.G., and Smith, D.G., 1990. *A Geologic Time Scale*: Cambridge (Cambridge Univ. Press).
- Head, M.J., and Norris, G., 1989. Palynology and dinocyst stratigraphy of the Eocene and Oligocene in ODP Leg 105 Hole 647A, Labrador Sea. In Srivastava, S.P., Arthur, M., Clement, B., et al., *Proc. ODP, Sci. Results*, 105: College Station, TX (Ocean Drilling Program), 515–550.
- Head, M.J., Norris, G., and Mudie, P.J., 1989a. Palynology and dinocyst stratigraphy of the upper Miocene and lowermost Pliocene, ODP Leg 105, Site 646, Labrador Sea. In Srivastava, S.P., Arthur, M., Clement, B., et al., *Proc. ODP, Sci. Results*, 105: College Station, TX (Ocean Drilling Program), 423–451.
- , 1989b. New species of dinocysts and a new species of acritarch from the upper Miocene and lowermost Pliocene, ODP Leg 105, Site 646, Labrador Sea. In Srivastava, S.P., Arthur, M., Clement, B., et al., *Proc. ODP, Sci. Results*, 105: College Station, TX (Ocean Drilling Program), 453–466.
- , 1989c. Palynology and dinocyst stratigraphy of the Miocene in ODP Leg 105, Hole 645E, Baffin Bay. In Srivastava, S.P., Arthur, M., Clement, B., et al., *Proc. ODP, Sci. Results*, 105: College Station, TX (Ocean Drilling Program), 467–514.
- Helby, R., Morgan, R., and Partridge, A.D., 1987. A palynologic zonation of the Australian Mesozoic. In Jell, P.A. (Ed.), *Studies in Australian Mesozoic Palynology*: Sydney (Assoc. Australas. Paleontol.), 1–85.
- Hertzog, R., 1979. Laboratory and field evaluation of an inelastic-neutron-scattering and capture gamma ray spectroscopy tool. *Soc. Pet. Eng. Pap.*, 7430.
- Jaeger, J.C., 1961. The effect of the drilling fluid on temperatures measured in boreholes. *J. Geophys. Res.*, 66:563–569.
- Kennett, J.P., and Srinivasan, S., 1983. *Neogene Planktonic Foraminifera*: Stroudsburg, PA (Hutchinson, Ross).
- Kvenvolden, K.A., and McDonald, T.J., 1986. *Organic Geochemistry on the JOIDES Resolution—An Assay*. ODP Tech. Note, 6.
- Lee, H.J., 1984. State of the art: laboratory determination of strength of marine soils. In Chaney, R.C., and Demars, K.R. (Eds.), *Strength Testing on Marine Sediments: Laboratory and In-situ Measurements*. ASTM Spec. Tech. Publ., 883:181–250.
- Lewis, D.W., 1984. *Practical Sedimentology*: Stroudsburg, PA (Hutchinson Ross).
- Lincoln, J.M., Pringle, M.S., and Premoli Silva, I., in press. Early and Late Cretaceous volcanism and reef-building in the Marshall Islands. In Pringle, M., Sager, W.W., Sliter, W.V., and Stein, S. (Eds.), *The Mesozoic Pacific*. Am. Geophys. Union, Geophys. Monogr. Ser.
- Lisitzin, A.P., Bogdanov, Y.A., Gurvitch, E.G., 1990. *Hydrothermal Deposits of Oceanic Rift Zones*: Moscow (Nauka).
- Manheim, F.T., and Sayles, F.L., 1974. Composition and origin of interstitial waters in marine sediments based on deep sea drill cores. In Goldberg, E.D. (Ed.), *The Sea* (Vol. 5): New York (Wiley-Interscience), 527–568.
- Manum, S.B., Boulter, M.C., Gunnarsdottir, H., Rangnes, K., and Scholze, A., 1989. Eocene to Miocene palynology of the Norwegian Sea (ODP Leg 104). In Eldholm, O., Thiede, J., Taylor, E., et al.,

- Proc. ODP, Sci. Results*, 104: College Station, TX (Ocean Drilling Program), 611–662.
- Martini, E., 1971. Standard Tertiary and Quaternary calcareous nannoplankton zonation. In Farinacci, A. (Ed.), *Proceedings of the Second International Conference on Planktonic Microfossils*, Roma: Rome (Ed. Technoscienza), 2:739–785.
- Matthews, D.J., 1939. *Tables of Velocity of Sound in Pore Water and in Seawater*: London (Admiralty, Hydrogr. Dept.).
- Mazzullo, J., and Graham, A.G. (Eds.), 1988. *Handbook for Shipboard Sedimentologists*. ODP Tech. Note, 8.
- Mazzullo, J.M., Meyer, A., and Kidd, R., 1988. New sediment classification scheme for the Ocean Drilling Program. In Mazzullo, J., and Graham, A.G. (Eds.), *Handbook for Shipboard Sedimentologists*. ODP Tech. Note, 8:45–67.
- McFadden, P.L., and Reid, A.B., 1982. Analysis of paleomagnetic inclination data. *Geophys. J.R. Astron. Soc.*, 69:307–319.
- Mudie, P.J., 1989. Palynology and dinocyst biostratigraphy of the late Miocene to Pleistocene, Norwegian Sea ODP Leg 104, Sites 642 to 644. In Eldholm, O., Thiede, J., Taylor, E., et al., *Proc. ODP, Sci. Results*, 104: College Station, TX (Ocean Drilling Program), 587–610.
- Munsell Soil Color Charts, 1971: Baltimore (Munsell Color).
- Norrish, K., and Hutton, J.T., 1969. An accurate X-ray spectrographic method for the analysis of a wide range of geological samples. *Geochim. Cosmochim. Acta*, 33:431–453.
- Okada, H., and Bukry, D., 1980. Supplementary modification and introduction of code numbers to the low-latitude coccolith biostratigraphic zonation (Bukry, 1973; 1975). *Mar. Micropaleontol.*, 5:321–325.
- Perch-Nielsen, K., 1985a. Mesozoic calcareous nannofossils. In Bolli, H.M., Saunders, J.B., and Perch-Nielsen, K. (Eds.), *Plankton Stratigraphy*: Cambridge (Cambridge Univ. Press), 329–426.
- _____, 1985b. Cenozoic calcareous nannofossils. In Bolli, H.M., Saunders, J.B., and Perch-Nielsen, K. (Eds.), *Plankton Stratigraphy*: Cambridge (Cambridge Univ. Press), 427–554.
- Pezard, P.A., Lovell, M., and Ocean Drilling Program Leg 126 Shipboard Scientific Party, 1990. Downhole images—electrical scanning reveals the nature of subsurface oceanic crust. *Eos*, 71:710, 718.
- Powell, A.J. (Ed.), 1990. *A Stratigraphic Index of Dinoflagellate Cysts*: London (Chapman and Hall), 290.
- Premoli Silva, I., and Brusa, C., 1981. Shallow-water skeletal debris and larger foraminifers from Deep Sea Drilling Project Site 462, western equatorial Pacific. In Larson, R.L., Schlanger, S.O., et al., *Init. Repts. DSDP*, 61: Washington (U.S. Govt. Printing Office), 439–474.
- Reynolds, R.C., 1967. Estimations of mass absorption coefficients by Compton scattering: improvements and extensions of the method. *Am. Mineral.*, 48:1133–1143.
- Rio, D., Fornaciari, E., and Raffi, I., 1990. Late Oligocene through Early Pleistocene calcareous nannofossils from western equatorial Indian Ocean (Leg 115). *Proc. ODP, Sci. Results*, 115: College Station, TX (Ocean Drilling Program), 175–235.
- Roth, P.H., 1978. Cretaceous nannoplankton biostratigraphy and oceanography of the northwestern Atlantic Ocean. In Benson, W.E., Sheridan, R.E., et al., *Init. Repts. DSDP*, 44: Washington (U.S. Govt. Printing Office), 731–759.
- Schaub, H., 1981. *Nummulites et Assilines de la Tethys paléogène*. Taxonomie, phylogénèse et biostratigraphie. *Mem. Suisses Paleontol.*, 104.
- Schlumberger, Inc., 1972. *Log Interpretation* (Vol. 1): *Principles*: New York (Schlumberger).
- Serra, O., 1984. *Fundamentals of Well Log Interpretation* (Vol. 1): *The Acquisition of Logging Data*: Amsterdam (Elsevier).
- Shepard, F.P., 1954. Nomenclature based on sand-silt-clay ratios. *J. Sediment. Petrol.*, 24:151–158.
- Shipboard Scientific Party, 1987. Site 645. In Srivastava, S., Arthur, M.A., et al., *Proc. ODP, Init. Repts.*, 105: College Station, TX (Ocean Drilling Program), 61–418.
- Sissingh, W., 1977. Biostratigraphy of Cretaceous calcareous nannoplankton. *Geol. Mijnbouw*, 56:37–65.
- Thierstein, H.R., 1971. Tentative Lower Cretaceous nannoplankton zonation. *Eclogae Geol. Helv.*, 64:458–488.
- _____, 1973. Lower Cretaceous calcareous nannoplankton zonation. *Abh. Geol. Bundesanst.*, 29:1–52.
- Timur, A., and Toksoz, M.N., 1985. Fundamentals of well log interpretation. *Annu. Rev. Earth Planet. Sci.*, 13:315–344.
- Vacquier, V., 1985. The measurements of thermal conductivity of solids with a transient liner heat source on the plane surface of a poorly conducting body. *Earth Planet. Sci. Lett.*, 74:275–279.
- van Gorsel, J.J., 1978. Late Cretaceous orbitoidal foraminifera. In Hedley, R.H., and Adams, C.G. (Eds.), *Foraminifera* (Vol. 3): London (Academic Press), 1–120.
- von Herzen, R.P., and Maxwell, A.E., 1959. The measurements of thermal conductivity of deep-sea sediments by a needle probe method. *J. Geophys. Res.*, 64:1557–1563.
- Wentworth, C.K., 1922. A scale of grade and class terms for clastic sediments. *J. Geol.*, 30:377–392.
- Williams, G.L., and Bujak, J.P., 1985. Mesozoic and Cenozoic dinoflagellates. In Bolli, H.M., Saunders, J.B., and Perch-Nielsen, K. (Eds.), *Plankton Stratigraphy*: Cambridge (Cambridge Univ. Press), 847–964.
- Zoback, M.D., Zoback, M.L., Mount, V.S., Suppe, J., Eaton, J.P., Healy, J.H., Oppenheimer, D., Reasenber, P., Jones, L., Raleigh, C.B., Wong, I.G., Scotti, O., and Wentworth, C., 1988. New evidence on the state of stress of the San Andreas Fault. *Science*, 238:1105–1111.

Ms 144IR-102